

## **Investigating the Physiological Relevance of *Ex Vivo* Disc Organ Culture Nutrient Microenvironments using *In-Silico* Modelling and Experimental Validation**

Emily E. McDonnell <sup>1,2</sup> and Conor T. Buckley <sup>1,2,3,4\*</sup>

<sup>1</sup> Trinity Centre for Biomedical Engineering, Trinity Biomedical Sciences Institute, Trinity College Dublin, The University of Dublin, Dublin, Ireland

<sup>2</sup> Discipline of Mechanical, Manufacturing and Biomedical Engineering, School of Engineering, Trinity College Dublin, The University of Dublin, Dublin, Ireland

<sup>3</sup> Advanced Materials and Bioengineering Research (AMBER) Centre, Royal College of Surgeons in Ireland & Trinity College Dublin, The University of Dublin, Dublin Ireland

<sup>4</sup> Tissue Engineering Research Group, Department of Anatomy and Regenerative Medicine, Royal College of Surgeons in Ireland, 121/122 St. Stephen's Green Dublin 2, Ireland

\*Corresponding author: Conor T. Buckley

E-mail address: conor.buckley@tcd.ie

Address: Trinity Centre for Biomedical Engineering

Trinity Biomedical Sciences Institute

Trinity College Dublin

Ireland

Telephone: +353-1-896-2061

**Key words:** degeneration, intervertebral disc, oxygen, glucose, pH, metabolism

**Running Header:** Modelling and characterisation of disc organ cultures

## **Abstract**

*Ex vivo* disc organ culture systems have become a valuable tool for the development and pre-clinical testing of potential intervertebral disc (IVD) regeneration strategies. Bovine caudal discs have been widely selected due to their large availability and comparability to human IVDs in terms of size and biochemical composition. However, despite their extensive use, it remains to be elucidated whether their nutrient microenvironment is comparable to human degeneration. This work aims to create the first experimentally validated *in-silico* model which can be used to predict and characterise the metabolite concentrations within *ex vivo* culture systems.

Finite element models of cultured discs governed by previously established coupled reaction-diffusion equations were created using COMSOL Multiphysics®. Experimental validation was performed by measuring oxygen, glucose and pH levels within discs cultured for 7 days, in a static compression bioreactor. The *in-silico* model was successfully validated through good agreement between the predicted and experimentally measured concentrations. For an *ex vivo* organ cultured in high glucose medium (4.5 g/L or 25mM) and normoxia, a larger bovine caudal disc (Cd1-2 to Cd3-4) had a central concentration of ~2.6 %O<sub>2</sub>, ~8 mM of glucose and a pH value of 6.7, while the smallest caudal discs investigated (Cd6-7 and Cd7-8), had a central concentration of ~6.5 %O<sub>2</sub>, ~12 mM of glucose and a pH value of 6.9.

This work advances the knowledge of *ex vivo* disc culture microenvironments and highlights a critical need for optimisation and standardisation of culturing conditions. Ultimately, for assessment of cell-based therapies and successful clinical translation based on nutritional demands, it is imperative that the critical metabolite values within organ cultures (minimum glucose, oxygen & pH values) are physiologically relevant and comparable to the stages of human degeneration.

## **Introduction**

*Ex vivo* disc organ culture models have become an important link between *in vitro* cell culture and *in vivo* studies for addressing fundamental research questions associated with disc degeneration<sup>1-9</sup> or for the assessment of regenerative cell therapies at an early stage of development.<sup>10-20</sup> These systems involve the long-term culturing of isolated discs from a variety of small and large animals, as well as cadaveric human intervertebral discs (IVD). They can provide a high-throughput platform, while refining and reducing animal studies and their associated financial and ethical burdens. An additional benefit is that the effect of specific treatment strategies can be investigated in a more controlled environment.<sup>21</sup> The popularity of *ex vivo* disc organ culture has grown over the past decade (Figure 1A) with the focus being either the development of bioreactor systems<sup>22-29</sup> or their utilisation to investigate degeneration processes<sup>1-9</sup> or regeneration strategies.<sup>10-20</sup> Discs from a variety of different species including mouse<sup>30,31</sup>, rat<sup>32,33</sup>, lapine<sup>1,34</sup>, bovine<sup>35-38</sup>, ovine<sup>39,40</sup>, caprine<sup>22,41</sup>, porcine<sup>24,42</sup> and human<sup>3,19</sup> have been used. Bovine caudal discs have become a widely accepted model for *ex vivo* disc organ culture as reflected by their popularity in published works (Figure 1B). Their attraction is heightened by their ease of isolation, high availability in large numbers and they have been shown to be comparable to human discs in terms of biochemical composition and the loss of notochordal cells following birth.<sup>43,44</sup>

Gantenbein *et al.* (2015) has compiled a comprehensive overview of disc organ culture bioreactor-platforms highlighting the different methods being used to establish degeneration or injury models.<sup>21</sup> More recent advances have been made to recapitulate the pro-inflammatory and catabolic niche associated with human degeneration through intradiscal injection or culture media supplementation of pro-inflammatory cytokines.<sup>23,45</sup> However, despite the promising development and increased complexity of disc organ culture, standardisation of *in vitro* and *in vivo* protocols is a hot topic across the research field. In addition, it has been well established that the harsh nutrient microenvironment within the disc provides a significant barrier for the

survival and regenerative potential of implanted cell treatments<sup>46-52</sup>, with the native *in vivo* microenvironment characterised by low concentrations of nutrients and increased matrix acidity.<sup>53,54</sup> While *in-silico* modelling has been used extensively to investigate nutrient transport in the human IVD<sup>55-63</sup>, to the best of our knowledge, a similar approach has never been applied to *ex vivo* disc organ culture systems.

It has been shown that low glucose availability results in decreased disc cell viability<sup>64</sup>, while oxygen is necessary for maintaining the disc specific extracellular matrix (ECM), with highest proteoglycan (PG) synthesis rates occurring at approximately 5 %O<sub>2</sub>. However, once the oxygen concentration falls below this level, synthesis appears to be inhibited significantly.<sup>65</sup> Additionally, hypoxia and the subsequent accumulation of lactate from glycolysis results in the progression of a pro-inflammatory microenvironment.<sup>66,67</sup> For *in vitro* cell culture, the *in vivo* disc nutrient microenvironment can be implemented simply by culturing cells in low oxygen, reduced glucose and serum and increased acidity.<sup>49,50,53,68,69</sup> However, ensuring a nutrient-deprived ECM in whole disc culture may require more consideration and sophistication. A number of recent *ex vivo* disc organ studies have combined mechanical loading with low glucose culture medium to induce a catabolic niche and pro-inflammatory cell response.<sup>11,15,23,35</sup> Another used short-term glucose deprivation before refreshing the medium with a higher concentration of glucose.<sup>37</sup> Pfannkuche *et al.* (2019) stated that the major challenge in the setup of organ culture is the maintenance of the anatomical integrity of the disc through retaining the cartilage endplate (EP) and adjacent vertebral bone, while still allowing adequate nutrition.<sup>70</sup> This is important as several studies suggest that the central region of the EP is the predominant pathway for nutrient diffusion into the nucleus pulposus (NP) and inner annulus fibrosis (AF), while more minor molecules are supplied via the AF.<sup>1,5,17</sup> However, the nutrient and metabolite concentrations within *ex vivo* models have never been measured and the assessment of adequate nutrition has typically been based on cell viability.

The vast majority of *ex vivo* studies have used Live/Dead staining as a viability indicator, while a smaller proportion have used a more specific test for metabolically active cells by assessing the mitochondrial activity using MTT (3-(4,5-Dimethyl-2-thiazolyl)-2,5-diphenyltetrazolium Bromide) combined with a nuclear counter stain.<sup>9,10,71–73</sup>

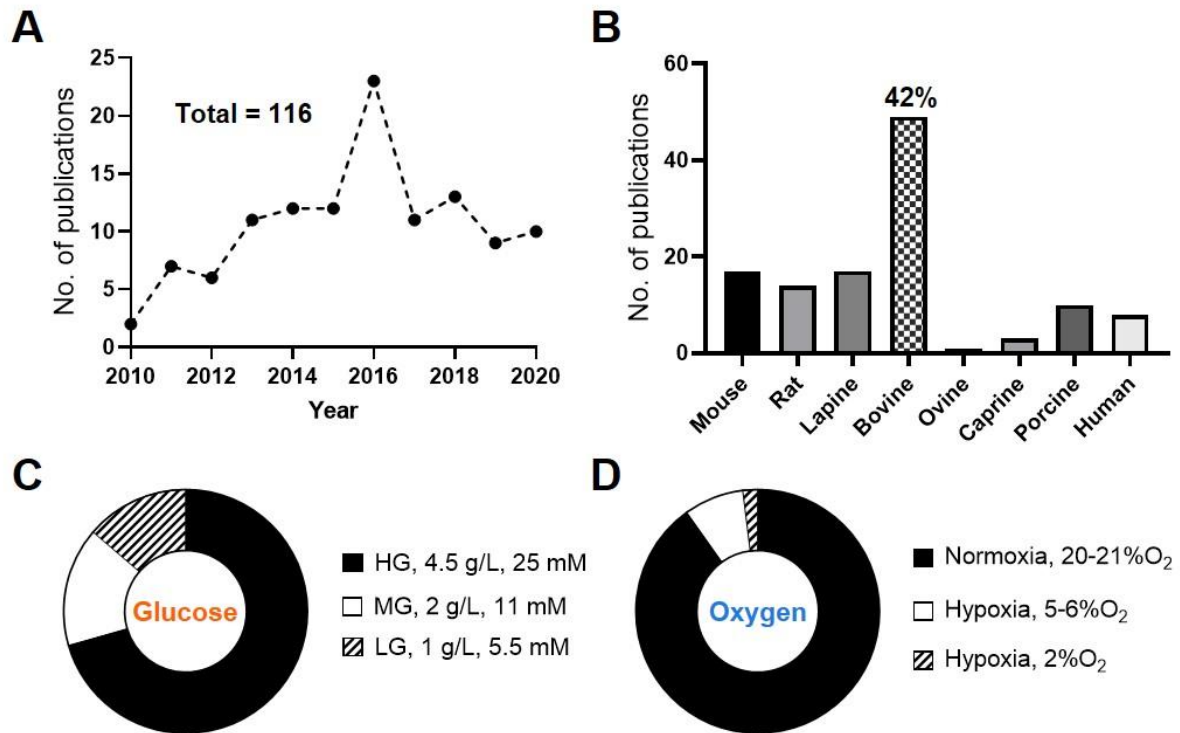


**Figure 1.** (A) *Ex vivo* disc organ culture systems have become an important platform in the disc research field with 116 papers published over the last decade. (B) Despite a variety of species being used, almost half of the publications used bovine caudal discs. (C) 70% of *ex vivo* discs are cultured in high glucose (HG), while 16% are cultured in medium glucose (MG) and 14% are cultured in low glucose (LG) medium. (D) 90% of *ex vivo* discs are cultured under normoxic conditions (20-21 % O<sub>2</sub>).

In terms of standardising *ex vivo* disc organ culture, it has been acknowledged that it is necessary to optimise parameters such as the loading force and frequency needed to model a physiological or degenerative impact on discs of different scales from different species.<sup>74</sup> However, it may also be necessary to refine the culturing medium based on disc parameters

such as species and disc size. For example, 70% of published *ex vivo* discs are cultured in high glucose (HG) medium (4.5 g/L or 25 mM) (Figure 1C), yet these discs range in scale from mouse to human lumbar IVDs and have significantly different disc heights and lateral widths.<sup>75</sup> As a result, the diffusional distance to the central NP cells would be significantly different between these models, and the local glucose concentration has never been measured in order to establish whether culturing in HG medium creates a physiologically relevant nutrient microenvironment. Less diversity is seen in the oxygen culturing conditions (Figure 1D), with the majority of research groups culturing in normoxia. However, a few studies have cultured in hypoxic or physioxic conditions.<sup>12,14</sup> Like glucose, the resulting oxygen level in the disc centre has never been quantifiably measured. Therefore, it is unknown whether these systems truly represent a physiologically relevant niche to test potential regenerative therapies based on nutritional demands.

This work aims to characterise the nutrient microenvironment of the most common *ex vivo* disc organ culture, bovine caudal discs cultured in HG medium and normoxia. Finite element models of cultured discs were created using COMSOL Multiphysics®. These models were governed by coupled reaction-diffusion equations, considering geometrical differences between caudal level and a metabolically active cell density. Metabolic rates were dependent on local oxygen and pH levels by employing equations derived previously.<sup>53,76</sup> Experimental verification of these models was performed by measuring the metabolite concentrations of oxygen, glucose and pH in discs cultured for 7 days.

## **Materials & Methods**

### ***Geometrical characterisation of disc caudal level***

Caudal discs were excised from six skeletally mature bovine tails (30 - 48 months). All bovine animal tissue used in this study was obtained from a local abattoir and did not require ethical

approval. The discs were removed from the vertebral bone using a mitre saw (Evolution Power Tools, UK) to cut proximally and distally to the EP retaining as little of the bony component as possible (Figure 2A). The discs were halved through the sagittal plane using a custom-made guillotine. Dimensions of the key diffusional distances (disc diameter, central NP thickness and overall disc height including bony EP) were measured for each caudal level (Figure 2B).

### ***Disc isolation and organ culture setup***

For organ culture, bovine tissue was obtained from a local abattoir within four hours of sacrifice. Discs were isolated as described above, under sterile conditions. Blood clots and bone debris were removed from the EP by flushing with phosphate buffered saline (PBS) containing 100 U/mL penicillin, 100 µg/mL streptomycin and 0.25 µg/mL amphotericin B (all Sigma-Aldrich, Ireland). Discs were placed into experimental groups based on their caudal level. The largest discs, Cd1-2 to Cd3-4, were placed into Group 1, Cd4-5 and Cd5-6 into Group 2 and the smallest discs, Cd6-7 and Cd7-8 into Group 3. To account for donor variance, each group consisted of three caudal discs from three different tails. Discs were cultured in 80 mL of HG Dulbecco's Modified Eagle Medium (4.5 g/L or 25 mM HG-DMEM, Thermo Fisher Scientific, UK) supplemented with 10% foetal bovine serum (FBS), 100 U/mL penicillin, 100 µg/mL streptomycin, 0.25 µg/mL amphotericin B, 1.5 g/mL bovine serum albumin (BSA) and 40 µg/mL L-proline (all Sigma-Aldrich, Ireland) and 0.1 mg/mL Primocin (Invivogen, France). Media was adjusted to ~400 mOSm using 150 mM sucrose (S0389, Sigma-Aldrich). The constraining effect on *ex vivo* disc organ culture systems has previously been described.<sup>12</sup> As a result, a custom-made bioreactor containing a compression spring with a rate of 8.92 N/mm (751-641, Radionics) was used to achieve ~0.4 MPa static loading (Figure 2C). The individual bioreactors were placed on an orbital shaker under gentle agitation (25 rpm) in a normoxia

incubator (37°C, ~20 %O<sub>2</sub> and ~5 %CO<sub>2</sub>). The culture period was seven days, with a complete media exchange performed halfway through the culture period.

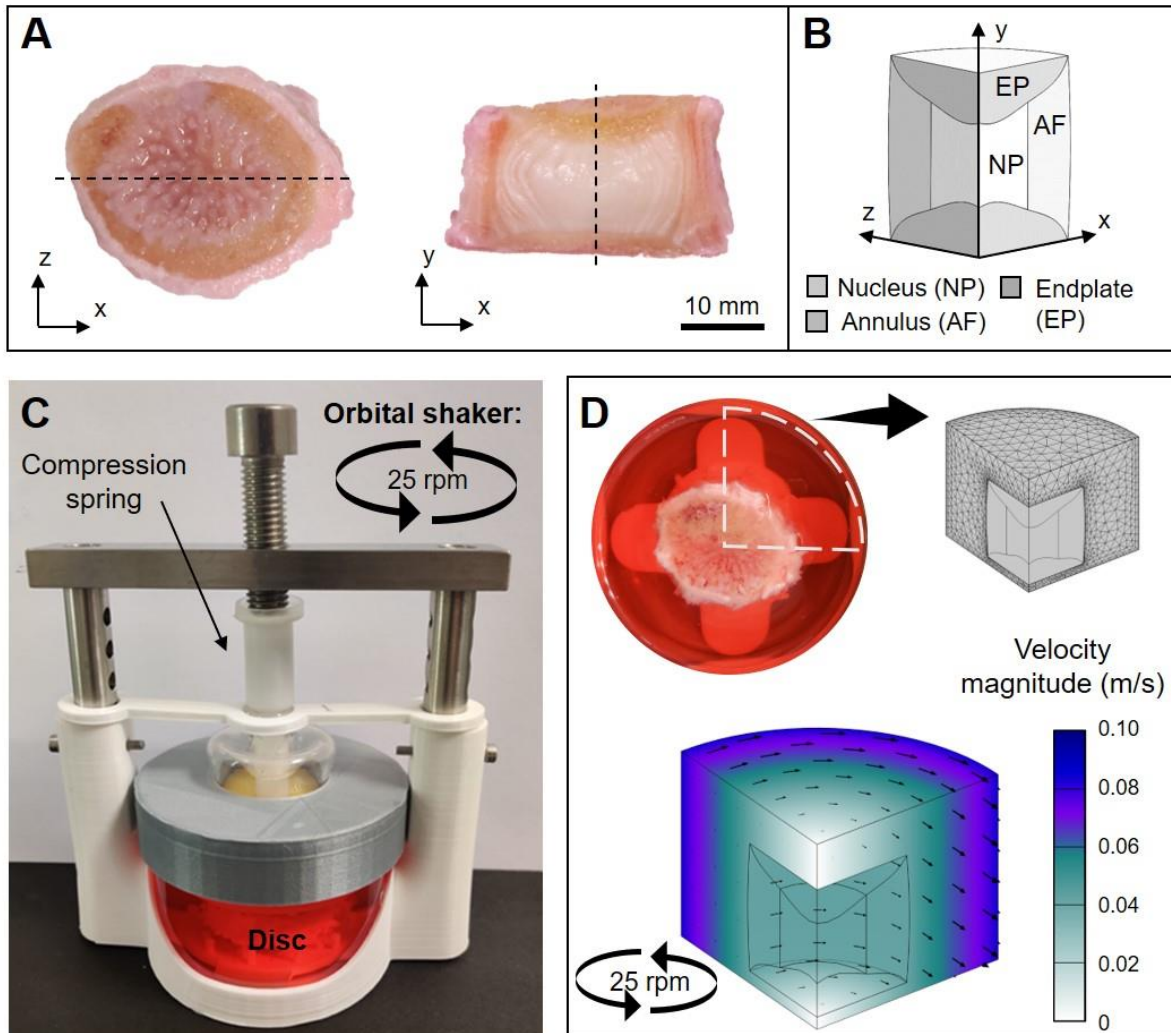


**Figure 2.** (A) Geometry of a bovine caudal disc from Group 2 (Cd4-5). (B) Assuming perfect symmetry, a disc quadrant was used for the *in-silico* simulations. (C) A custom-made bioreactor containing a screw and a compression spring was developed which applies a physiologically relevant static load of ~ 0.4 MPa to the cultured disc. The bioreactor is placed on an orbital shaker at a speed of 25 rpm. (D) Each disc was cultured in 80 mL of media. The rotational flow in the media domain was modelled to mitigate any oxygen gradient and ensure mixing of glucose/lactate throughout the media.



***Determining metabolically active cell density***

A metabolically active cell density at day 0 and day 7 was determined using the MTT (3-(4,5-Dimethylthiazol 2-yl)-2,5-diphenyltetrazolium bromide) assay and DAPI (4',6-diamidino-2-phenylindole) (both Sigma-Aldrich, Ireland) counterstaining as previously described.<sup>71-73</sup> Freshly isolated and cultured discs were cut in half along the sagittal plane and an approximate 3 mm thick section was taken across the full diameter of the disc. The sections were incubated in high-osmolarity phenol-free DMEM with 0.5 mg/mL MTT for three hours under gentle agitation at 37°C. Tissue was washed, embedded in Optimal Cutting Temperature (OCT) compound and stored at -80°C until sectioning on a cryotome. For cell density analysis, 10 µm slices were cut, randomly selected for mounting on a microscope slide using fluoroshield with DAPI. Slides were examined under both brightfield, to capture active MTT+ cells, and fluorescence, to capture all cell nuclei stained with DAPI (Olympus BX51 upright microscope). The metabolically active proportion was assessed qualitatively by merging the brightfield and DAPI image using ImageJ (National Institutes of Health, and Bethesda, Maryland). Images for the NP and AF regions at day 0 and day 7 can be found in Supplementary Figure S1. The total number of cells (DAPI) was determined automatically while the number of dual stained cells (overlapping formazan crystals and blue nuclei) was performed manually using the cell counter plug-in.

***Experimental measurements of oxygen, pH and glucose***

Following culture, the metabolite concentrations (oxygen, glucose and pH) were measured in the centre of each disc. The intradiscal oxygen and pH levels were measured using fibre-optical fluorescent microsensors (PreSens, Regensburg, Germany). To ensure confidence in the measurement techniques, both microsensors were calibrated and the accuracy of the glucose assay tested before use. The oxygen microprobe underwent a two-point calibration at 0% and

100% air saturation. These calibration points were created by saturating the medium with nitrogen gas and compressed air, respectively. The pH sensor is pre-calibrated by the manufacturer from pH 4 to pH 8. The pH probe was also validated over a range of pH 6 to 8. During measurements, the sensor probe was placed into pH 7 buffer before and between each disc measurement to ensure accurate and consistent measurement throughout. The discs were maintained in their culture medium at 37°C during the analysis, with the attached temperature sensor placed in the medium. Discs were rotated onto their sides to enable the insertion of a needle, containing the microsensor tip, into the disc centre (Supplementary Figure S2). Oxygen measurements were taken until the concentration changed by < 0.1% between sampling times for a two-minute period. This was established as an acceptable equilibrium criterion while limiting the measuring time to less than ten minutes for each disc. Glucose was measured biochemically by taking 2 mm biopsies from the centre of the NP (~ 12.5 mm<sup>3</sup>). To determine the water content, wet and dry tissue weights were recorded before and after lyophilisation. Samples were digested with 3.88 U/mL papain in 0.1 M sodium acetate, 5 mM L-cysteine HCl, and 0.05 M EDTA (all from Sigma–Aldrich, Ireland) at 60°C under constant agitation for 18 hours. The total glucose content of the digested sample was quantified using an enzymatic-colorimetric assay (Sentinel Diagnostics, Italy), which was then normalised to the water content of the original tissue samples to obtain a concentration (mol/L). Glucose concentration and pH level of the culture media were also determined. The glucose assay was validated for both media samples and digested tissue samples of a known glucose concentration. The tissue samples were created by soaking biopsies in a known concentration of glucose until they were fully equilibrated.

### ***In-silico model of nutrient concentration profiles***

A 3-D anatomical disc model was created for each of the three experimental groups based on the results of the geometrical characterisation (Figure 2A-B). Symmetry was assumed in the x- and y-plane (Figure 2A) to simplify the model to a quadrant of the full disc with three distinct tissue domains: NP, AF and EP (Figure 2B). In order to simulate the transport of metabolites between the culture media and the disc, a quadrant of the surrounding media was incorporated. The *in-silico* model was created using COMSOL Multiphysics 5.5 (COMSOL Inc., Burlington, USA). The media domain incorporated a pseudo-stationary rotational flow to capture the mixing from the orbital shaker (Figure 2D). Dilute species transport based on Fick's Law was applied across all domains for oxygen, glucose and lactate (pH). The *in-silico* model was governed by coupled reaction-diffusion equations accounting for the metabolically active cell population and metabolite diffusion parameters through the different domains (Table 1). Metabolic rates were modelled as being dependent on local oxygen and pH levels by employing equations derived and published previously.<sup>53</sup> Oxygen consumption rate (OCR) was modelled using Michaelis-Menten kinetics. Huang *et al.* have used the Michaelis-Menten equation to describe the functional relationship between OCR and both oxygen concentration and pH level<sup>76,77</sup>:

$$Q^{O_2} = - \frac{V_{max}(pH - 4.95)C^{O_2}}{K_m(pH - 4.59) + C^{O_2}} \rho_{cell} \quad (1)$$

where  $Q^{O_2}$  is the consumption rate ( $\mu\text{M/hr}$ ),  $t$  is the time (hr),  $C^{O_2}$  is the local oxygen concentration ( $\mu\text{M}$ ),  $pH$  is the local pH level and  $\rho_{cell}$  is the cell density (million cell/mL).  $V_{max}$  is the maximum consumption rate (nmol/million cells/h) and  $K_m$  is the rate limiting Michaelis-Menten constant i.e. the oxygen concentration ( $\mu\text{M}$ ) at which the consumption rate is at half its maximum. The rate of lactate production ( $Q^{lac}$ ), which is exponentially dependent on local pH and oxygen levels, was also based on that of bovine NP cells from the literature<sup>53</sup>:

$$Q^{lac} = \exp(-2.47 + 0.93 \times pH + 0.16 \times C^{O_2} - 0.0058 \times C^{O_2^2}) \rho_{cell} \quad (2)$$

The rate of glucose consumption ( $Q^{gluc}$ ) was incorporated based on the assumption that disc cell metabolism is primarily glycolytic, a process where one molecule of glucose is broken down to produce two molecules of lactate. Therefore, glucose consumption was simply modelled as:

$$Q^{gluc} = -0.5 \times Q^{lac} \quad (3)$$

The pH level in the disc model was calculated from the lactate concentration based on an approximately linear relationship established from experimental data<sup>53,78</sup>:

$$pH = A \times C^{lac} + B \quad (0 < C^{lac} < 30 \text{ mM}) \quad (4)$$

where  $A = -0.1 \text{ mM}^{-1}$  and  $B = 7.5^{76}$ .

### ***Statistical analysis***

One-way or two-way ANOVA were used for analysis of variance using GraphPad Prism (version 8). Tukey's multiple comparisons test was used to compare between groups. Results are displayed as mean  $\pm$  standard deviation, where n represents the number of biological replicates. Specifically, in the case of the cell density analysis, each biological replicate had 6 technical replicates. Significance was accepted at a level of  $p < 0.05$ .

**Table 1. Input parameters and boundary conditions used in the *in-silico* models for nucleus pulposus (NP), annulus fibrosus (AF), endplates (EP) and media.**

		NP	AF	EP	Media
Active cell density (cells/mm <sup>3</sup> )	<i>Day 0</i>	5,500 <sup>a</sup>	17,000 <sup>a</sup>	-	-
	<i>Day 7</i>	5,500 <sup>a</sup>	4,200 <sup>a</sup>	-	-
Michaelis-Menten constants	<i>Vmax (nmol/million cells/hr)</i>			-	-
	<i>Km (μM)</i>	5 <sup>b</sup>	6 <sup>c</sup>		
Effective diffusion coefficient (mm <sup>2</sup> /hr)	<i>D<sub>glucose</sub></i>	1.35 <sup>d</sup>	0.9 <sup>d</sup>	0.76 <sup>e</sup>	2.22 <sup>f</sup>
	<i>D<sub>oxygen</sub></i>	5 <sup>d</sup>	3.78 <sup>d</sup>	2.18 <sup>e</sup>	9.36 <sup>g</sup>
	<i>D<sub>lactate</sub></i>	2.28 <sup>e</sup>	1.45 <sup>e</sup>	1.13 <sup>e</sup>	4.32 <sup>h</sup>
Boundary (culturing) conditions	<i>Glucose (mM)</i>	-	-	-	20.9 <sup>a</sup>
	<i>Oxygen (%O<sub>2</sub>)</i>	-	-	-	18.6 <sup>i</sup>
	<i>Lactate (mM)</i>	-	-	-	1.6 <sup>a</sup>

<sup>a</sup> Values determined experimentally in this work.

<sup>b</sup> Experimentally determined for freshly isolated gel encapsulated bovine NP cells<sup>53</sup>.

<sup>c</sup> Experimentally determined for freshly isolated gel encapsulated porcine AF cells<sup>77</sup>.

<sup>d</sup> Values used previously in the literature<sup>55,57,58</sup>.

<sup>e</sup> Values used previously in the literature<sup>62</sup>.

<sup>f</sup> Experimentally measured glucose diffusion in culture medium<sup>101</sup>.

<sup>g</sup> Experimentally calculated oxygen diffusion in culture medium<sup>102</sup>.

<sup>h</sup> Experimentally calculated lactose diffusion in aqueous solution<sup>103</sup>.

<sup>i</sup> True oxygen concentration in a normoxic incubator at sea level<sup>104</sup>.

## **Results**

### ***Geometrical variation of bovine discs as a function of caudal level***

Discs were categorised into groups based on their caudal level (Figure 3A). Significant differences were found between the disc diameters of all groups ( $p = 0.0072$ ), with this dimension decreasing with increasing caudal level (Figure 3B). The overall disc height incorporated the thickness of the bony EP above and below the disc tissue. This distance was  $27.5 \pm 1.9$  mm for Group 1,  $21.1 \pm 1.8$  mm for Group 2 and  $17.2 \pm 0.8$  mm for Group 3 ( $n = 6$ ). Differences were also observed between the central NP thickness of each group ( $12.6 \pm 0.5$  mm for Group 1,  $9.9 \pm 0.5$  mm for Group 2 and  $8.3 \pm 1.0$  mm for Group 3 ( $n = 6$ )) (Figure 3B).

### ***Metabolically active cell density of ex vivo disc organ cultures is an important input parameter for in-silico modelling***

The metabolically active cell density of the NP and AF regions was determined using MTT with a DAPI counterstain (Figure 3C, D). The total cell density (DAPI) and metabolically active cell density (MTT+) in the NP showed no significant differences across the control and experimental groups ( $n = 3$ ). The NP control (day 0) had a metabolically active cell population of approximately 93%, while this value ranged from 78 – 81% across the groups at day 7 (Figure 3E shows the total and MTT+ cell densities, calculated positive percentage is not presented). However, as no statistical significance was determined compared to the native control ( $p = 0.2738$  for Group 1,  $p = 0.1292$  for Group 2 and  $p = 0.1522$  for Group 3), a change in the total number of metabolically active cells in the NP domain was not considered in the *in-silico* model. The AF control (day 0) had a lower metabolically active cell population of approximately 86%, which appeared to reduce dramatically across the groups by day 7 (Figure 3F), with a significant difference determined between the total and active cell density in Group

2 ( $p = 0.0483$ ). The metabolically active cell density of the AF appeared to decline to a baseline comparable with the active cell density of the NP. As a result, the metabolically active cell density in the AF domain of the *in-silico* model was not assumed to be constant and changed in line with the experimental results (Table 1). In addition, no significant difference in total or active cell density was found between the experimental groups based on caudal level.

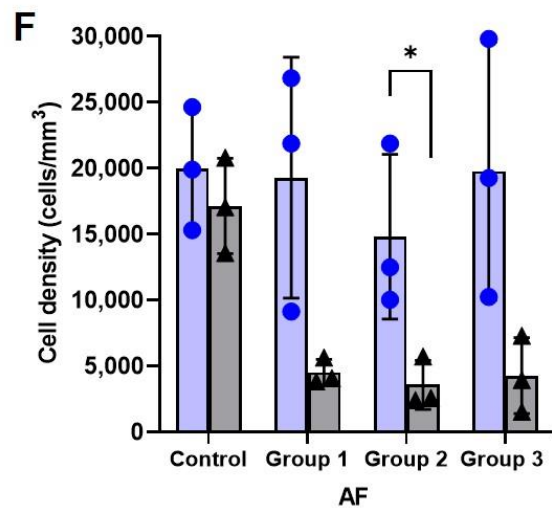
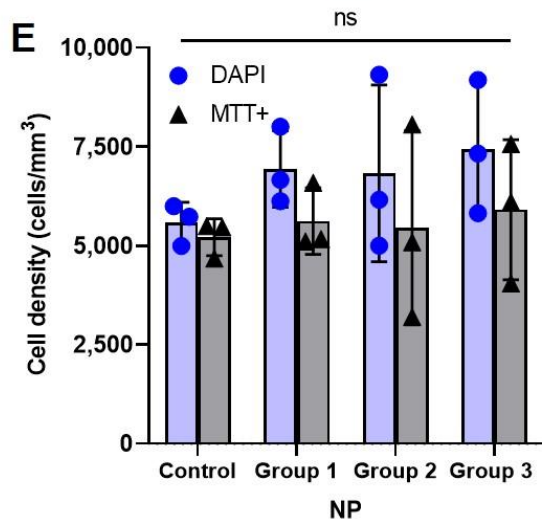
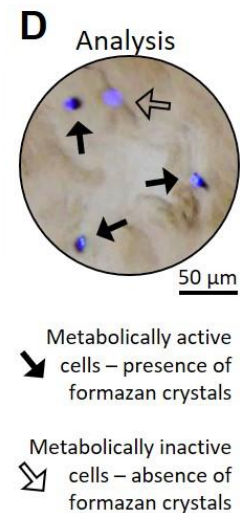
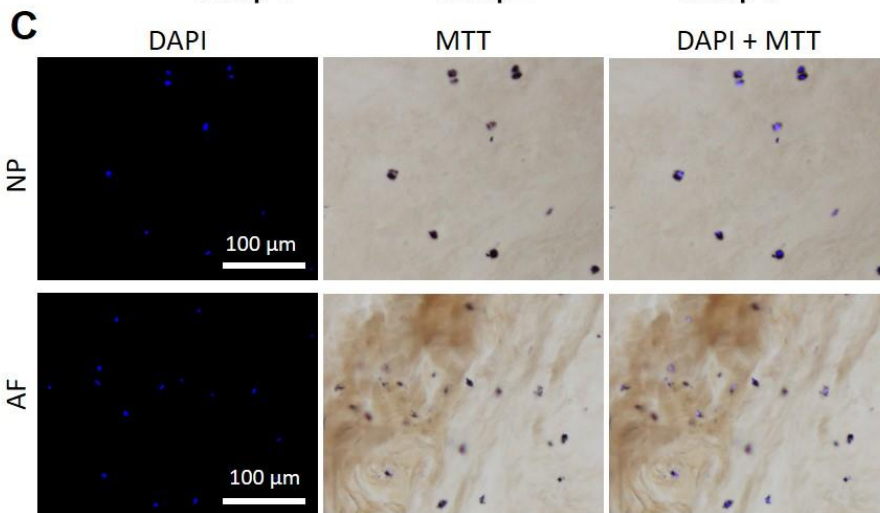
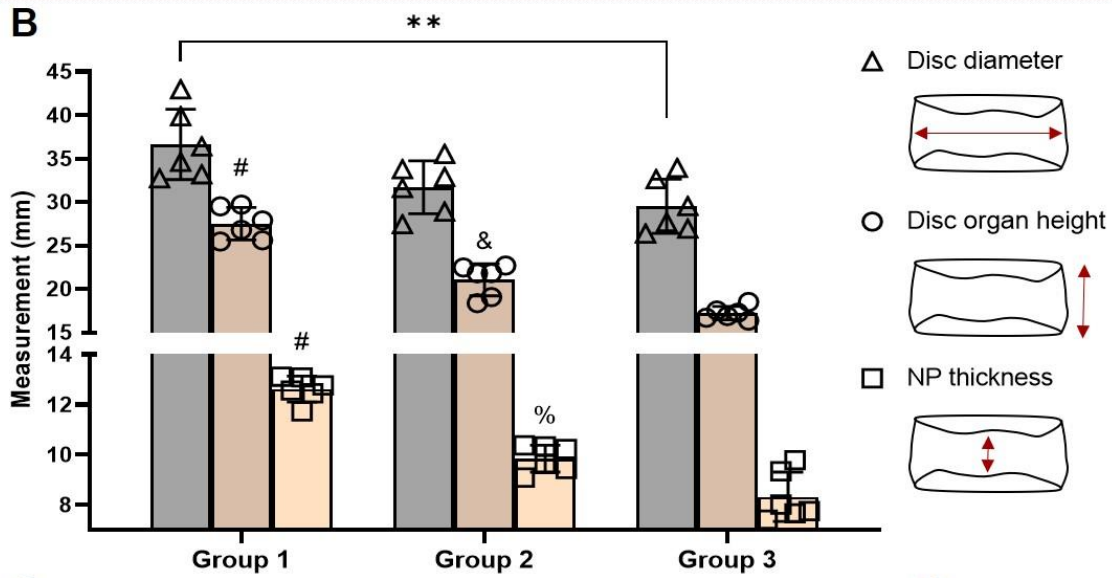
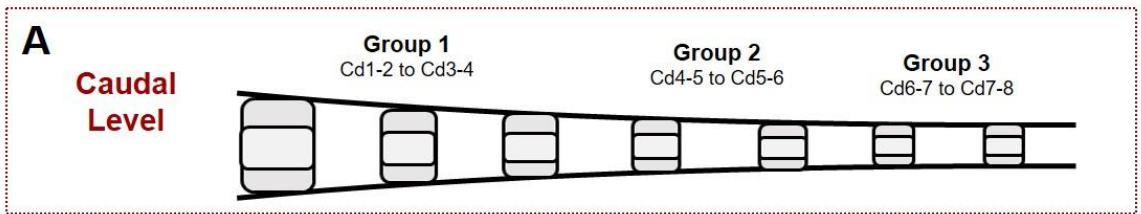




**Figure 3.** (A) Discs were categorised into three experimental groups based on bovine caudal disc level. Group 1: Cd1-2 to Cd3-4, Group 2: Cd4-5 and Cd5-6, Group 3: Cd6-7 and Cd7-8. (B) Key dimensions relating to nutrient transport distances across the three groups (n = 6). \*\* (p = 0.0072). # (p < 0.0001) indicates significance as compared to the same parameter in both Group 2 and Group 3 and & (p = 0.0020) and % (p = 0.0058) indicates significance as compared to corresponding parameter in Group 3. (C) DAPI images identifying the fluorescing blue nuclei of all cells in the NP and AF regions. MTT brightfield images show deposited formazan crystals around metabolically active cells. (D) Merging of the fluorescence and bright field images enabled identification of metabolically active and inactive cells. (E) The total cell density (DAPI) and metabolically active cell density (MTT+) determined in the NP of native (control) and Groups 1-3 after 7 days of culture (n = 3). No significance (ns) was found for NP regions. (F) The total cell density (DAPI) and metabolically active cell density (MTT+) determined in the AF of native (control) and Groups 1-3 after 7 days of culture (n = 3). \* (p = 0.0483).

***Predicted and experimentally determined metabolite concentrations in ex vivo bovine caudal discs***

As expected, oxygen decreased with distance from the boundary of the EP and periphery of the AF (Figure 4A, B). The steepest oxygen gradient was observed for the largest caudal disc (Group 1), which had the lowest oxygen concentration in the NP. The *in-silico* model predicted central oxygen concentrations were 1.4 %O<sub>2</sub> for Group 1, 2.5 %O<sub>2</sub> for Group 2 and 4.6 %O<sub>2</sub> for Group 3 (Figure 4B). The predicted central oxygen concentration for each group was compared with those determined experimentally within cultured caudal discs (Figure 4C). The experimentally measured values of oxygen were 2.6 ± 1.2 %O<sub>2</sub> for Group 1, 2.6 ± 0.3 %O<sub>2</sub> for Group 2 and 6.5 ± 4.6 %O<sub>2</sub> for Group 3 (n = 3), with no statistical difference between the

groups. However, there was a trend of increasing oxygen concentration within discs of decreased disc volume (i.e. Group 3 compared to Group 1) and the predicted values lie within the standard deviation of those determined experimentally. Overall, there was a 70% reduction from the oxygen level of the culture media to the centre of the *ex vivo* disc organ culture.

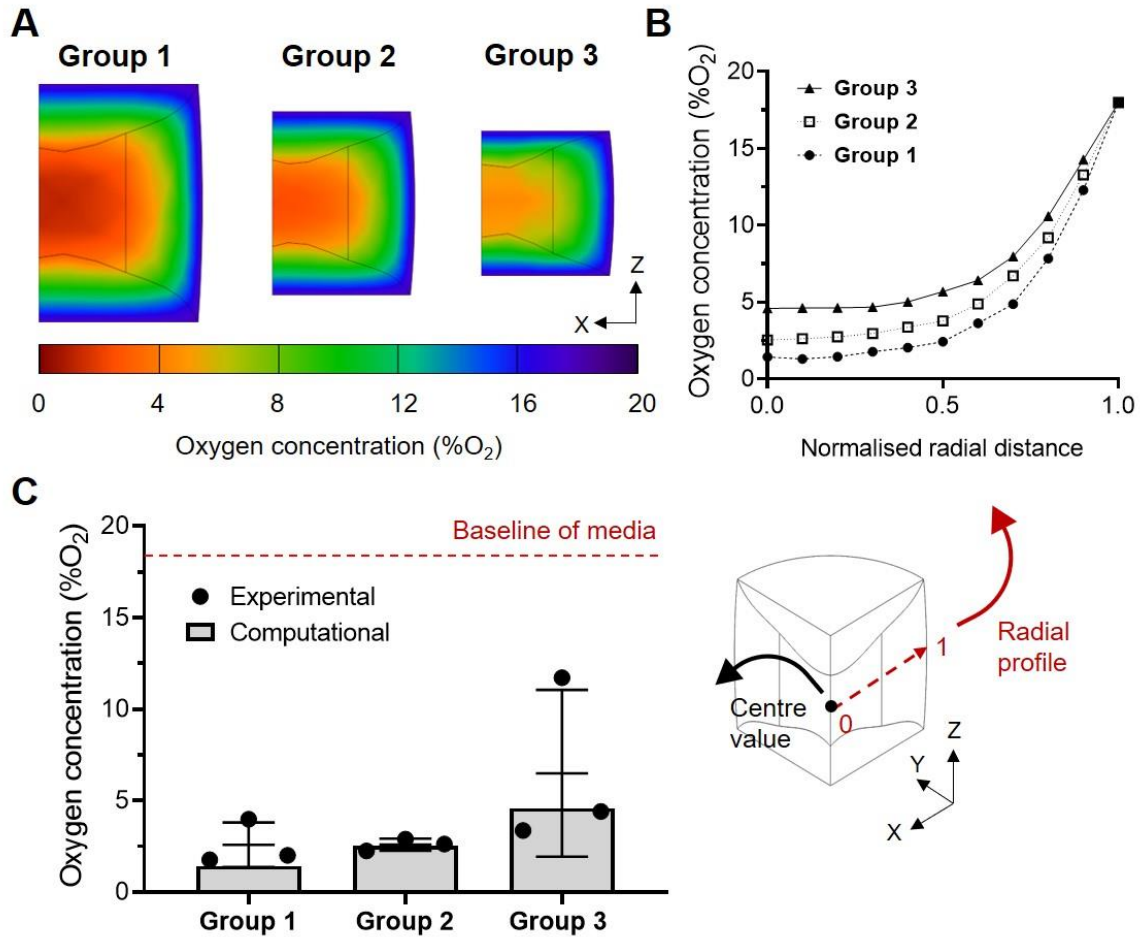


**Figure 4.** (A) Oxygen contour plots in the sagittal plane through the disc centre of each of the three groups. (B) Radial oxygen profile for the different groups. Starting in the disc centre (0.0) and ending at the disc periphery (1.0) (bottom right schematic). The radial distance was normalised by the disc diameter of each group. (C) Comparison of predicted *in-silico* model oxygen concentrations in the disc centre to experimentally measured values (n = 3). No statistical significance was found between the experimental groups.

The steepest gradient in glucose concentration was observed for Group 1, which had the lowest glucose concentration in the disc centre, while Group 3 had the highest concentration (Figure 5A, B). Predicted central values of glucose were 9.8 mM, 12.6 mM and 15.5 mM for Groups 1, 2 and 3, respectively (Figure 5B). The experimentally measured values of glucose were  $8.0 \pm 3.1$  mM for Group 1,  $10.6 \pm 4.5$  mM for Group 2 and  $12.0 \pm 4.3$  mM for Group 3 ( $n = 3$ ) (Figure 5C) and compared favourably with the *in-silico* model predictions. No statistical significance was found between the groups. However, as was the case for oxygen, there was a strong trend of increasing glucose concentration within discs of decreased disc volume, with the initial culturing concentration of glucose reducing approximately 62% in the NP of discs from Group 1 and approximately 25% in the NP of discs from Group 3. The predicted values were found to lie within the standard deviation of those determined experimentally.

In terms of pH, Group 1 had the highest build-up of acidity, while Group 3 exhibited the least acidic NP region with predicted central pH values of 6.75, 6.89 and 6.97 for Groups 1, 2 and 3, respectively (Figure 6A, B). The experimentally measured values of pH were  $6.72 \pm 0.01$  for Group 1,  $6.83 \pm 0.10$  for Group 2 and  $6.91 \pm 0.03$  for Group 3 ( $n = 3$ ) (Figure 6C). A significant difference was found between the experimentally measured pH value in the centre of Group 1 and Group 3 ( $p = 0.0221$ ). The predicted value for Group 2 lay within the standard deviation of the experimental results. Like the oxygen and glucose results, there was good agreement between the *in-silico* and experimental pH measurements.

### **Additional validation of the *in-silico* model through media analysis**

In order to further validate the *in-silico* model and strengthen the confidence in the predicted results, the glucose concentrations and pH levels in the culture media at day 7 were also analysed (Figure 7). Experimentally determined glucose concentrations in the media (Group 1:  $16.4 \pm 1.4$  mM, Group 2:  $17.6 \pm 1.2$  mM and Group 3:  $17.6 \pm 1.1$  mM,  $n=3$ ) were found to

compare favourably with the *in-silico* model predictions (Figure 7A, B). Similarly, experimentally determined pH values of the media were  $7.02 \pm 0.06$ ,  $7.13 \pm 0.06$  and  $7.17 \pm 0.05$  for Group 1, Group 2 and Group 3, respectively ( $n = 3$ ) (Figure 7C, D). Overall, the results of the media analysis revealed very close agreement between the *in-silico* models and experimental measurements.

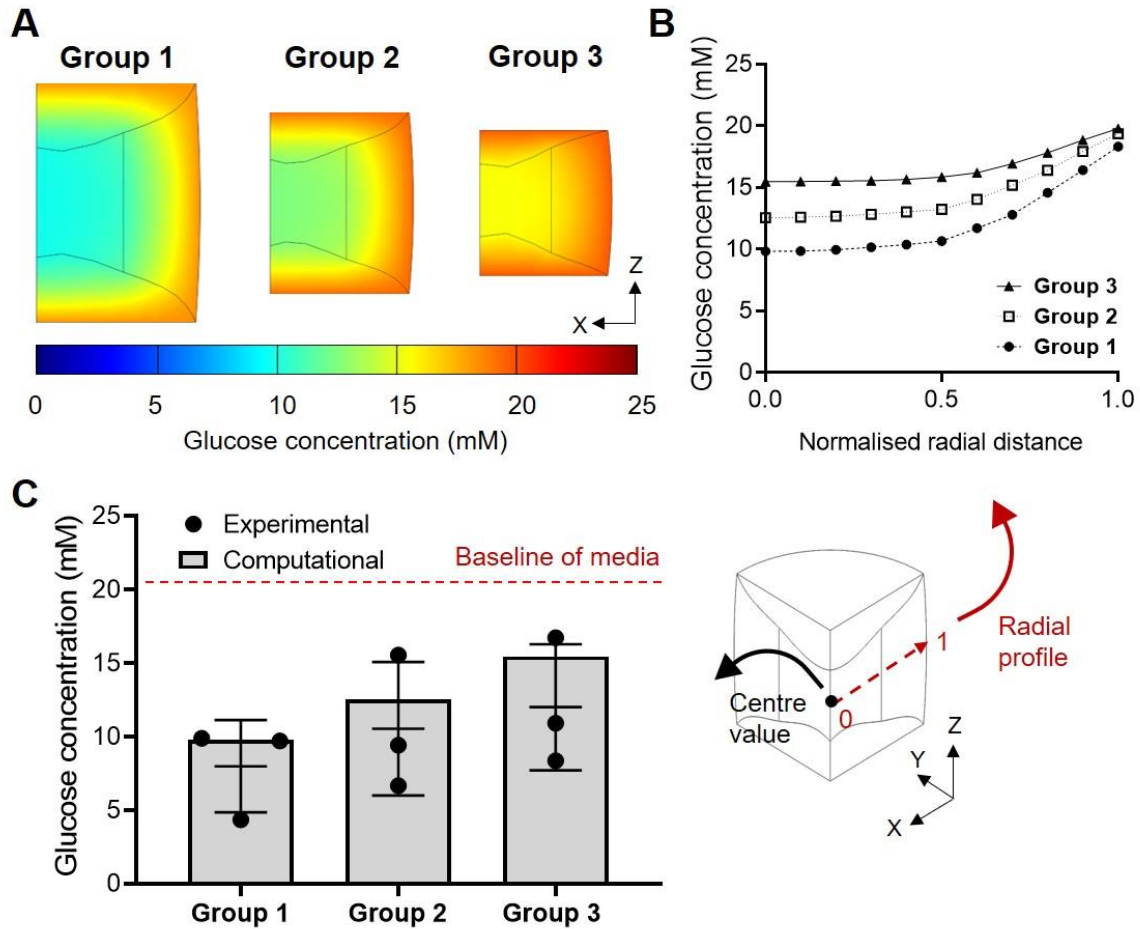


**Figure 5.** (A) Glucose contour plots in the sagittal plane through the disc centre of each of the three groups. (B) Radial glucose profile for the different groups. Starting in the disc centre (0.0) and ending at the disc periphery (1.0) (bottom right schematic). The radial distance was normalised by the disc diameter of each group. (C) Comparison of predicted *in-silico* model glucose concentrations in the disc centre to experimentally measured values ( $n = 3$ ). No statistical significance was found between the experimental groups.

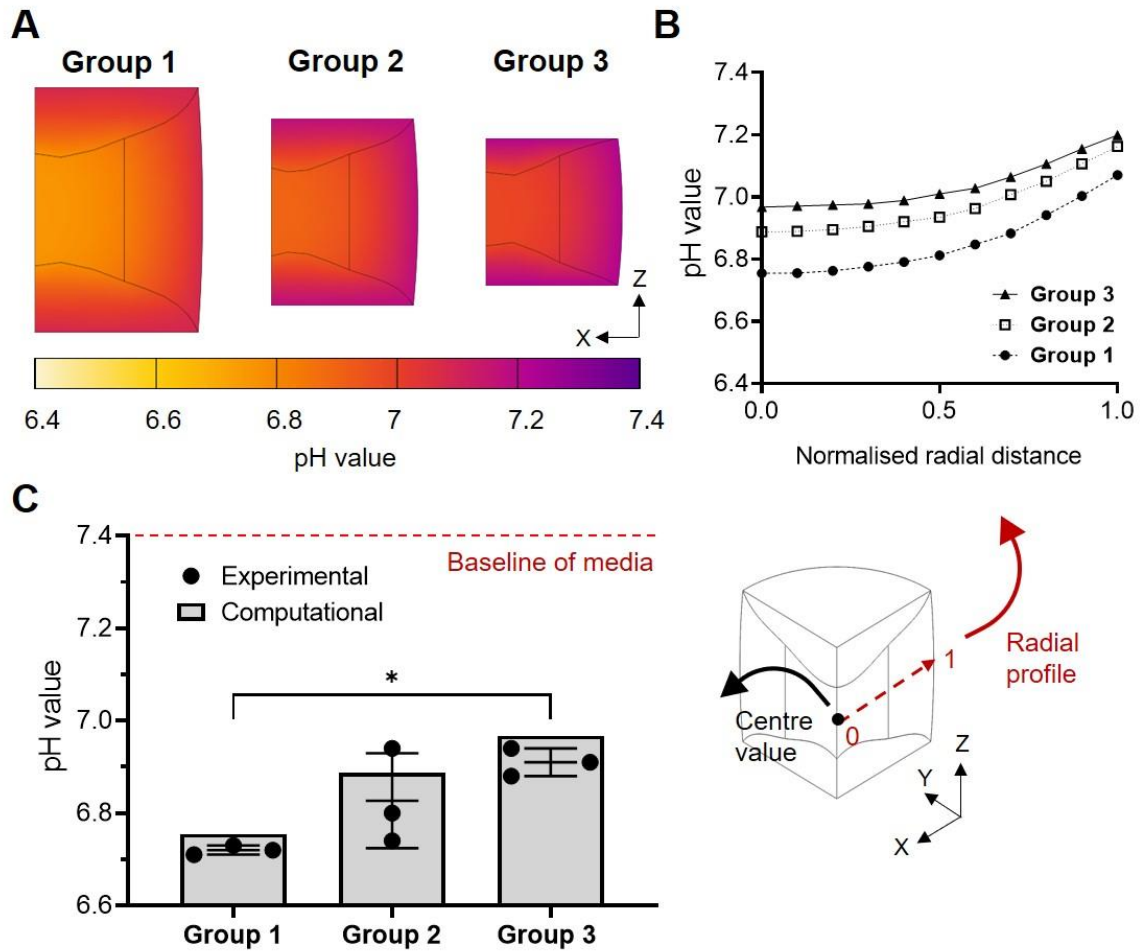


**Figure 6.** (A) pH contour plots in the sagittal plane through the disc centre of each of the three groups. (B) Radial pH profile for the different groups. Starting in the disc centre (0.0) and ending at the disc periphery (1.0) (bottom right schematic). The radial distance was normalised by the disc diameter of each group. (C) Comparison of predicted *in-silico* model pH values in the disc centre to experimentally measured values (n = 3). \* (p = 0.0221) indicates significance between Group 1 and Group 3.

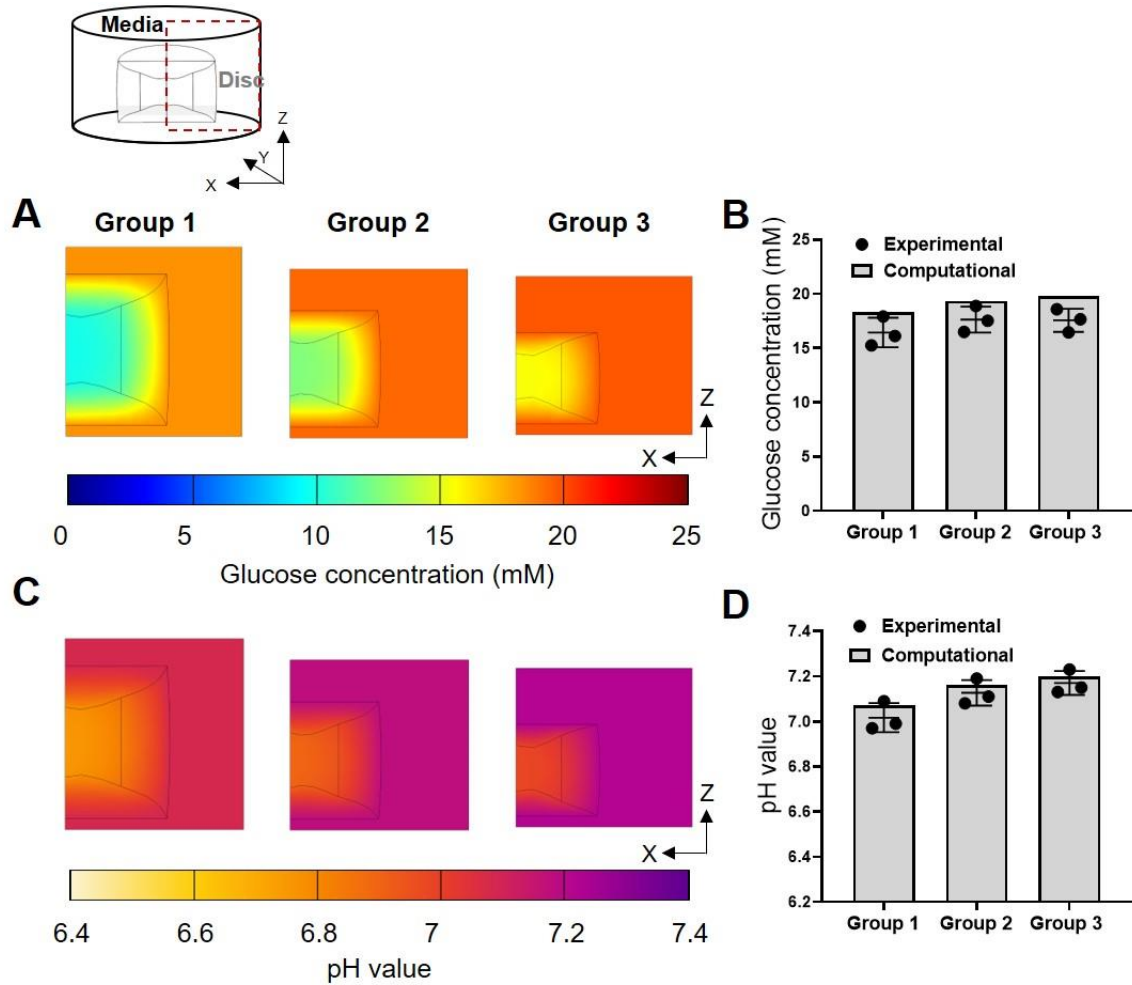


**Figure 7.** (A) Glucose contour plots in the sagittal plane through the disc centre and the surrounding media of each of the three groups. (B) Comparison of predicted glucose concentration in the culture media compared to experimentally measured values at day 7 ( $n = 3$ ). (C) pH contour plots in the sagittal plane through the disc centre and the surrounding media of each of the three groups. (D) Comparison of predicted pH values in the culture media compared to experimentally measured values at day 7 ( $n = 3$ ).

## **Discussion**

It has been well established that the harsh nutrient microenvironment of a degenerating IVD provides a significant barrier for the survival and regenerative potential of implanted cell treatments.<sup>49,50,53,68,69</sup> However, despite the attractiveness of *ex vivo* disc organ culture for the testing and evaluation of potential cell- and biomaterial-based strategies<sup>11,13–15,37</sup>, the nutrient microenvironment has never been quantitatively measured and, as a result, their clinical and physiological relevance to human, based on nutrient demands, has not been established. Therefore, this study aimed to characterise the metabolite microenvironments within *ex vivo* disc organ culture using the first experimentally validated *in-silico* nutrient transport model.

While HG medium is most commonly used for culturing *ex vivo* disc organ models<sup>9,11,18,36,38,73,79–87</sup>, the results of this study suggests that HG culturing creates suprphysiological levels in the disc centre (8 – 12 mM) when compared to predicted *in vivo* glucose concentrations of 0.2 – 1.9 mM under degenerative conditions.<sup>55–63</sup> An important distinction between *in vivo* and *ex vivo* nutrition is the pathway of nutrient transport. While the EP transport route appears to be the more predominant supply route for the NP physiologically, in *ex vivo* culture the blood vessels surrounding the AF and penetrating the EP have been removed and instead the disc is fully submerged in nutrient-rich medium. Thus, it is speculated that more radial nutrient diffusion occurs than exists *in vivo*, contributing further to the suprphysiological levels of glucose measured. This study measured an average oxygen concentration ~ 2.5 %O<sub>2</sub> in larger discs and ~ 6 %O<sub>2</sub> in smaller discs. In terms of hypoxia, these values could be considered markedly different, particularly when low oxygen is essential for NP cells to maintain their phenotype and disc-specific ECM production.<sup>65</sup> However, it is important to note that a study measuring oxygen in the IVD of patients suffering from lower back pain found considerable variation, with values ranging from 3.8 – 13.2 %O<sub>2</sub> in the centre of IVDs from the lumbar levels L3-4 and L4-5.<sup>54</sup> This study found a correlation between disc

height and pH level, with the largest discs having a significantly lower pH (~ 6.7) than the smallest (~ 6.9) ( $p = 0.0221$ ). This is shown for both the predicted and the experimental results, with the predicted contour plots highlighting the gradient of acidity in the larger discs. This correlation is important to note as several studies have used bovine discs of different sizes and caudal levels under the same culturing conditions.<sup>18,79,80</sup> An early study by Nachemson (1969) measured pH values of ~ 6.9 in lumbar IVDs of patients suffering from less severe levels of back pain and ~ 6.7 in patients suffering from severe backpain.<sup>88</sup> Therefore, the current *ex vivo* disc organ culture model appears to create a physiologically relevant central pH microenvironment. However, the disc size should be carefully considered based on the severity of the model desired in order to achieve the most appropriate acidic niche. Ultimately, it is imperative that the metabolite microenvironment established in culture is matched to the *in vivo* microenvironment at a stage of human degeneration where the regenerative therapy is being considered an appropriate strategy in a clinical context.

This study highlights that there is a need for standardisation of culturing conditions in order to reduce the *in vitro* to *in vivo* gap and realise more successful clinical translation based on nutritional demands. This is particularly important for interpretation of results when investigating the effect of cell-based therapies.<sup>11,18</sup> Hence, based on the results of this study, it could be conceivably hypothesised that differences in the microenvironment of *ex vivo* organ cultures may account for the mixed results in terms of cell survival and regenerative capacity of potential treatments. Some studies have utilised short term nutrient deprivation to elicit a degenerative response.<sup>37</sup> However, if there is diminished cell viability it is speculated that nutrient concentrations will most likely rise above physiological levels when returned to HG medium due to a subsequently reduced glycolytic metabolism. This study suggests that in order to achieve physiologically relevant levels of glucose in the centre of *ex vivo* disc organ systems, there is a need to reduce the culturing concentration, while central oxygen and pH levels appear



to be more comparable to the *in vivo* human condition. However, Jünger *et al.* (2009) observed significant reduction in the viability of bovine *ex vivo* discs due to limited glucose when cultured with an external glucose concentration of 2 g/L (11 mM) compared to HG media.<sup>20</sup> Although the current study showed no significant difference in the active NP cell density at day 7, the local glucose concentration was supraphysiological (~ 10 mM) and not comparable to the effect of a 'lower' glucose concentration. Therefore, there is an additional challenge of balancing a physiologically relevant glucose microenvironment while maintaining viability of *ex vivo* discs for long term culture. As this study observed a diminished metabolically active cell population in the AF region after culture, a sensitivity analysis was performed to assess AF viability as a key parameter. The results showed that even if the proportion of metabolically active cells remains high, the oxygen and glucose levels do not significantly reduce, and importantly the central glucose concentration remains supraphysiological (Supplementary Figure S3). However, a higher proportion of metabolically active cells predicted an increased acidity in the centre of the disc. Therefore, it is important to bear in mind that not only will the species disc size impact the local microenvironment and concentration gradients established, but also, the metabolically active cell density and specific metabolic rates.

Tissue composition such as the species-specific bone density and EP thickness and calcification will affect the solute transport in and out of the IVD.<sup>59,89-91</sup> However, in the case of this model the bovine caudal discs were absent of calcification and good agreement between experimental and predicted results suggest that the diffusion coefficients used to represent nutrient transport through the bovine EP with a segment of vertebral bone attached, in the *in-silico* model, were sufficiently representative of the physical organ culture. As mentioned previously, due to the culturing regime of *ex vivo* systems there is a shift in the supply routes. This may lessen the impact of solute transport effects due to variations in species-specific bone density, EP thickness, calcification or the presence of growth plate which can be found in young

animal disc organs. Despite different species having varying PG content, nutrients such as glucose and oxygen are uncharged molecules and should diffuse into the IVD at their route specific diffusion rates regardless of PG concentration.<sup>43,92</sup> This is supported by relatively similar glucose diffusion coefficients having been measured in both bovine and human disc tissue which have different PG content.<sup>93,94</sup> Additionally, sensitivity analysis of the *in-silico* model showed that the effective diffusion coefficients to be the least influential parameter, with cell density and cell demand playing the most important role in establishing the nutrient concentration gradients.

The geometrical analysis matched results of a previous study investigating the effect of bovine caudal disc height on NP cell density (calculated from DNA level) of freshly isolated discs.<sup>95</sup> Similarly, Boubriak *et al.* (2013) also found no significance between the cell density of different caudal levels or sagittal disc height. However, the authors stated large variation in absolute cell density from tail to tail, which was also reflected in the large standard deviation of the AF cell density of the current study. A study investigating age- and degeneration-related variation in cell density demonstrated human AF cell density decreasing from ~ 38,500 cells/mm<sup>3</sup> in the first year of life to ~ 1,600 cells/mm<sup>3</sup> after 30 to 60 years. Similarly, the degeneration effect highlights an AF cell density of ~ 25,500 cells/mm<sup>3</sup> at Grade I (infant) and ~ 5,000 cells/mm<sup>3</sup> at Grade IV.<sup>19</sup> Therefore, the higher bovine cell densities determined in this study appear to be more comparable to young and healthy or non-degenerated human IVDs. However, an unanticipated finding was the significant reduction in metabolically active cells in the AF after 7 days of culture, while the cells of the NP exhibited no significant difference compared with the native density. The bioreactor used was a relatively simple static compression system compared with some of the more established bioreactors across the research field which use dynamic-loading and physiological diurnal loading.<sup>21,70</sup> A possible explanation for the poor metabolic activity in the AF region may be due to constant

compression of the disc, where the pressure created in the NP is balanced by tensile stresses in the lamella of the AF. A recent study, providing support for this hypothesis, found a significant reduction in viable cells (lactate dehydrogenase staining) in the inner and outer AF after severe static compressive loading.<sup>96</sup> However, the effects of dynamic loading and fluid flow on solute transport in avascular tissues and constructs has not been fully elucidated. A key early *in vivo* study looking at the effects of physiological loads and fluid transport on tracer concentrations found that fluid “pumping” during movement had an insignificant effect on small solutes such as oxygen and glucose.<sup>97</sup> However, due to the shift in nutrient supply routes this may be different for *ex vivo* bioreactor systems and warrants further investigation.

As with any *in-silico* model, there are certain limitations and assumptions. Within the scope of this study it was not possible to determine our own metabolic rates for bovine tissue. While OCRs have been reported for bovine NP cells<sup>53</sup>, none have been reported for AF cells. Therefore, it was assumed that the Michaelis-Menten constants for bovine AF cells were comparable with those reported for porcine AF cells.<sup>77</sup> Cell density and metabolism rates will significantly impact the nutrient concentration profiles and are dependent on the species. For the purposes of accurately predicting nutrient concentration profiles it is important to determine the metabolically active cell population (using the MTT method or similar) as opposed to conventional Live/Dead indicators. The metabolism rates of cells appear to vary between species and degeneration. For example, rat and rabbit NP cells have been shown to exhibit higher lactate production rates compared to non-notochordal bovine NP cells.<sup>98</sup> In addition degenerated human cells exhibit 3 – 5 times greater OCR than non-degenerated cells.<sup>99</sup> Unfortunately, due to the mechanics of MTT staining it is only possible to capture a binary indication of cell activity. However, several studies have investigated disc cell metabolism at a range of physiological and supraphysiological glucose concentrations.<sup>11,21–25</sup> In general, significant cell death appears to occur below a glucose threshold of 0.5 mM (for more than 3

days) and disc cells have shown little difference in glucose consumption rate between 1 and 5 mM.<sup>22,26,27</sup> Additionally, previous work has typically shown higher glucose and lower oxygen consumption at supraphysiological glucose levels.<sup>11,21,23,25</sup> Taken together, it is critically important to understand the species-specific metabolically active cell density and metabolism rates in order to achieve a physiologically relevant microenvironmental niche through optimising the nutrient boundary conditions of *ex vivo* organ culture. However, given the good agreement between the *in-silico* concentrations and those measured experimentally, any computational simplifications and assumptions appear justified. As a result of successful validation, the current model could be used to predict the culturing conditions necessary to tailor a desired nutrient microenvironment using key input parameters such as species-specific rates of metabolism, metabolically active cell density and disc geometry. Additionally, it could be developed further to model the impact of delivering cells into a degenerated disc model, as well as identifying an optimal cell number to sustain viability without adversely affecting the local nutrient microenvironment. Despite promising characterisation of the metabolite microenvironment of a relatively straightforward *ex vivo* disc organ culture system, more work is needed to experimentally characterise the effect of introducing pro-inflammatory cytokines on the nutrient microenvironment and cellular metabolism.<sup>23,45</sup> A recent agent-based model has shown promising advancement in *in-silico* modelling by developing an inflammation and mRNA expression sub-model to capture cellular behaviour in a more multifactorial, biochemical environment.<sup>100</sup> Significant advancements in *ex vivo* disc organ culture have also identified optimal loading force and frequency of more complex bioreactor systems.<sup>74</sup> Importantly, it has been acknowledged that such parameters must be identified and optimised between discs of different species and scale.<sup>70</sup> The findings of this work suggest that a similar approach is needed in terms of optimising the nutrition of *ex vivo* disc organ culture systems based on geometrical differences. Combining advanced *in-silico* modelling with experimental

validation offers a powerful tool for the standardisation of *ex vivo* disc organ culture systems and refinement of animal models. Taken together, this approach offers the ability to better predict the *in vivo* human events and outcomes accelerating the development of cell-based therapeutics towards clinical translation.

## **Conclusion**

Organ culture systems offer unparalleled advantages for the development and preclinical testing of new regenerative strategies. However, the findings of this work suggest that further optimisation and standardisation of *ex vivo* disc organ culture is needed to recapitulate the *in vivo* microenvironmental niche of a degenerating human IVD. Although high glucose and normoxic conditions are the most commonly used culturing conditions across all species of *ex vivo* disc organ culture, this study found supraphysiological levels of glucose exist in the centre of bovine caudal discs under these conditions. While the choice of species may be dependent on the specific scientific question, if the nutrient microenvironment is relevant to the study aim, then the culturing parameters may need to be optimised based on disc geometry, metabolically active cell density and species-specific metabolism. Once standardised, it is anticipated that these systems will provide a more powerful and reliable platform to test new treatments and accelerate innovative therapeutics for clinical translation.

## **Acknowledgements**

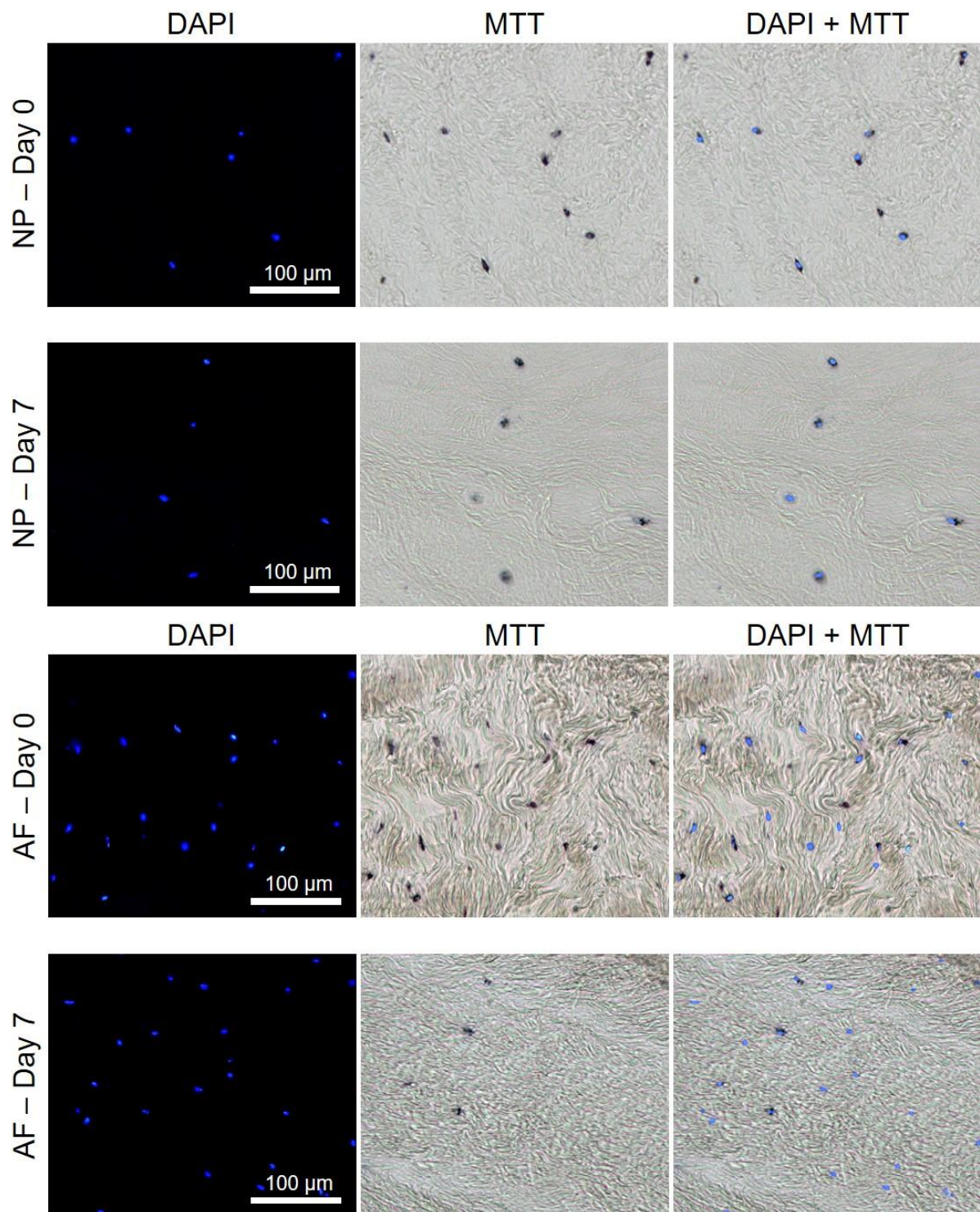
This work was supported by the Irish Research Council (IRC) - Government of Ireland Postgraduate Scholarship Scheme (GOIPG/2018/2448) and Science Foundation Ireland Career Development Award (15/CDA/3476).

## **Conflicts of Interest**

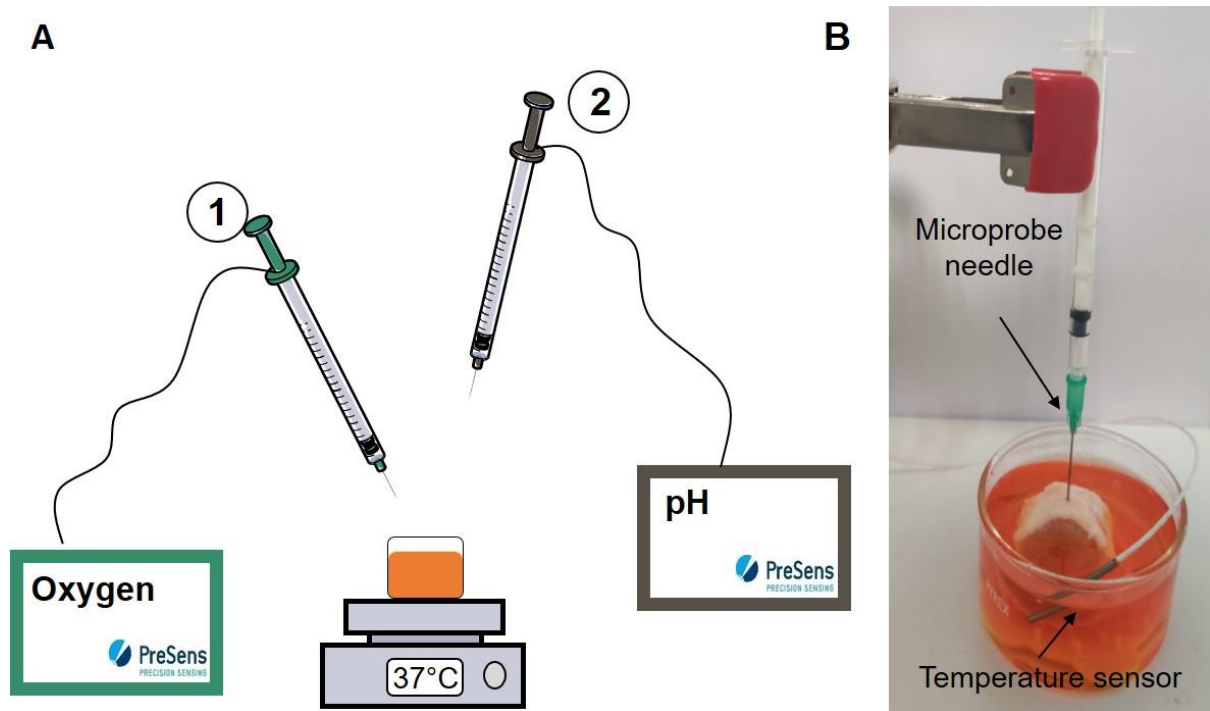
The authors declare no conflicts of interest.

**Authors Contribution**

Emily McDonnell provided substantial contribution to study design, data acquisition and computational modelling, data analysis and presentation, interpretation of data, drafting of the article, revising it critically and final approval. Conor Buckley is the overall project funding holder, takes responsibility for the integrity of the work as a whole from inception to finalised article, provided substantial contributions to study design, data presentation, interpretation of data, drafting of the article, revising it critically, and final approval.

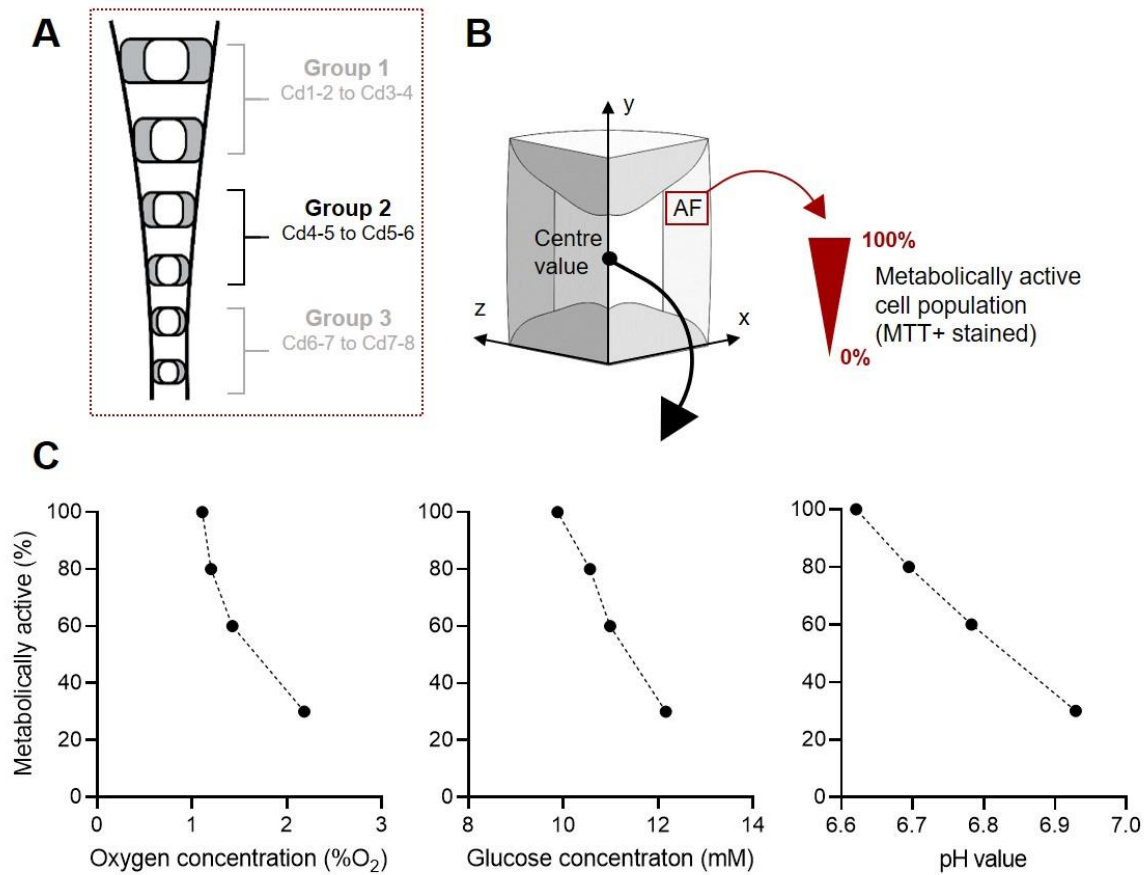


**Supplementary Figure S1.** DAPI images identifying the fluorescing blue nuclei of all cells in the nucleus pulposus (NP) and annulus fibrosus (AF) at day 0 and day 7. MTT brightfield images showing deposited formazan crystals around metabolically active cells. Merging of the fluorescence and bright field enabled identification of metabolically active (dual stained) and inactive cells (blue only). Scale bar is 100 µm.



**Supplementary Figure S2.** (A) Schematic of the probe measurement setup. The discs were kept at 37°C in their culture dish and media during the analysis. The oxygen probe was used first to avoid the measurement being compromised by any air which may enter the disc after the needle is withdrawn. (B) The disc was turned onto its side so that the insertion point of the needle was above the surface of the media and the needle was inserted a distance half of the disc diameter. Both the oxygen and the pH sensor have a coupled temperature sensor which was placed into the media during the analysis.





**Supplementary Figure S3.** (A) The *in-silico* model for Group 2 (Cd4-5 and Cd5-6) was used to exemplify the effect of metabolically active cell density as an influential parameter on the central metabolite concentrations. (B) As the experimental results revealed a reduction in the metabolically active cell density of the annulus fibrosus (AF), a sensitivity analysis was performed for this domain only. (C) The central oxygen concentration increased by ~ 1 %O<sub>2</sub>, while the central glucose concentration only increased by ~ 2 mM for a 70% reduction in metabolically active cells. However, a higher metabolically active cell population predicted a notably more acidic pH in the disc centre.

## References

1. Zhan JW, Wang SQ, Feng MS, et al. Constant compression decreases vascular bud and VEGFA expression in a rabbit vertebral endplate ex vivo culture model. *PLoS One*. 2020. doi:10.1371/journal.pone.0234747
2. Choi H, Chaiyamongkol W, Doolittle AC, et al. COX-2 expression mediated by calcium-TonEBP signaling axis under hyperosmotic conditions serves osmoprotective function in nucleus pulposus cells. *J Biol Chem*. 2018. doi:10.1074/jbc.RA117.001167
3. Krock E, Rosenzweig DH, Currie JB, Bisson DG, Ouellet JA, Haglund L. Toll-like receptor activation induces degeneration of human intervertebral discs. *Sci Rep*. 2017;7(1):1-12. doi:10.1038/s41598-017-17472-1
4. Pang L, Li P, Zhang R, Xu Y, Song L, Zhou Q. Role of p38–MAPK pathway in the effects of high-magnitude compression on nucleus pulposus cell senescence in a disc perfusion culture. *Biosci Rep*. 2017. doi:10.1042/BSR20170718
5. Li P, Gan Y, Wang H, et al. Role of the ERK1/2 pathway in osmolarity effects on nucleus pulposus cell apoptosis in a disc perfusion culture. *J Orthop Res*. 2017. doi:10.1002/jor.23249
6. Walter BA, Likhitpanichkul M, Illien-Junger S, Roughley PJ, Hecht AC, Iatridis JC. TNF $\alpha$  transport induced by dynamic loading alters biomechanics of intact intervertebral discs. *PLoS One*. 2015. doi:10.1371/journal.pone.0118358
7. Krock E, Rosenzweig DH, Chabot-Doré AJ, et al. Painful, degenerating intervertebral discs up-regulate neurite sprouting and CGRP through nociceptive factors. *J Cell Mol Med*. 2014. doi:10.1111/jcmm.12268
8. Markova DZ, Kepler CK, Addya S, et al. An organ culture system to model early degenerative changes of the intervertebral disc II: Profiling global gene expression changes. *Arthritis Res Ther*. 2013. doi:10.1186/ar4301

9. Purmessur D, Walter BA, Roughley PJ, Laudier DM, Hecht AC, Iatridis J. A role for TNF $\alpha$  in intervertebral disc degeneration: A non-recoverable catabolic shift. *Biochem Biophys Res Commun.* 2013;433(1):151-156. doi:10.1016/j.bbrc.2013.02.034
10. Richards J, Tang S, Gunsch G, et al. Mast cell/proteinase activated receptor 2 (PAR2) mediated interactions in the pathogenesis of discogenic back pain. *Front Cell Neurosci.* 2019;13(July):1-14. doi:10.3389/fncel.2019.00294
11. Wangler S, Menzel U, Li Z, et al. CD146/MCAM distinguishes stem cell subpopulations with distinct migration and regenerative potential in degenerative intervertebral discs. *Osteoarthr Cartil.* 2019;27(7):1094-1105. doi:10.1016/j.joca.2019.04.002
12. Teixeira GQ, Boldt A, Nagl I, et al. A Degenerative/Proinflammatory Intervertebral Disc Organ Culture: An Ex Vivo Model for Anti-inflammatory Drug and Cell Therapy. *Tissue Eng Part C Methods.* 2016;22(1):8-19. doi:10.1089/ten.tec.2015.0195
13. Naqvi SM, Gansau J, Gibbons D, Buckley CT. In Vitro Co-culture and Ex Vivo Organ Culture Assessment of Primed and Cryopreservation Stromal Cell. *Eur Cells Mater.* 2019;37:134-152.
14. Teixeira GQ, Pereira CL, Ferreira JR, et al. Immunomodulation of Human Mesenchymal Stem/Stromal Cells in Intervertebral Disc Degeneration. *Spine (Phila Pa 1976).* 2018;43(12):E673-E682. doi:10.1097/BRS.0000000000002494
15. Peroglio M, Douma LS, Caprez TS, et al. Intervertebral disc response to stem cell treatment is conditioned by disc state and cell carrier: An ex vivo study. *J Orthop Transl.* 2017;9:43-51. doi:10.1016/j.jot.2017.03.003
16. Anderson DG, Markova D, An HS, et al. Human Umbilical Cord Blood Y Derived Mesenchymal Stem Cells in the Cultured Rabbit Intervertebral Disc A Novel Cell Source for Disc Repair. *Am J Phys Med Rehabil.* 2013;92(5):420-429.

- doi:10.1097/PHM.0b013e31825f148a
17. Illien-Jünger S, Pattappa G, Peroglio M, et al. Homing of mesenchymal stem cells in induced degenerative intervertebral discs in a whole organ culture system. *Spine (Phila Pa 1976)*. 2012;37(22):1865-1873. doi:10.1097/BRS.0b013e3182544a8a
  18. Chan SCW, Gantenbein-Ritter B, Leung VYL, Chan D, Cheung KMC, Ito K. Cryopreserved intervertebral disc with injected bone marrow-derived stromal cells: a feasibility study using organ culture. *Spine J*. 2010;10(6):486-496. doi:10.1016/j.spinee.2009.12.019
  19. Rosenzweig DH, Gawri R, Moir J, et al. Dynamic loading, matrix maintenance and cell injection therapy of human intervertebral discs cultured in a bioreactor. *Eur Cells Mater*. 2016. doi:10.22203/eCM.v031a03
  20. Mwale F, Wang HT, Roughley P, Antoniou J, Haglund L, Link N and mesenchymal stem cells can induce regeneration of the early degenerate intervertebral disc. *Tissue Eng - Part A*. 2014;20(21-22):2942-2949. doi:10.1089/ten.tea.2013.0749
  21. Gantenbein B, Illien-Jünger S, Chan SCW, et al. Organ culture bioreactors-platforms to study human intervertebral disc degeneration and regenerative therapy. *Curr stem cell Res Ther*. 2015;10(4):339-352. <http://www.pubmedcentral.nih.gov/articlerender.fcgi?artid=4437861&tool=pmcentrez&rendertype=abstract>.
  22. Rustenburg CME, Snuggs JW, Emanuel KS, et al. Modelling the Catabolic Environment of the Moderately Degenerated Disc with a Caprine Ex Vivo Loaded Disc Culture System. *Eur Cells Mater*. 2020;40:21-37. doi:10.22203/eCM.v040a02
  23. Lang G, Liu Y, Gerjes J, et al. An intervertebral disc whole organ culture system to investigate proinflammatory and degenerative disc disease condition. *J Tissue Eng Regen Med*. 2018;12(4):e2051-e2061. doi:10.1002/term.2636

24. Li P, Gan Y, Wang H, et al. A Substance Exchanger-Based Bioreactor Culture of Pig Discs for Studying the Immature Nucleus Pulposus. *Artif Organs*. 2017.  
doi:10.1111/aor.12834
25. Li Z, Lezuo P, Pattappa G, et al. Development of an ex vivo cavity model to study repair strategies in loaded intervertebral discs. *Eur Spine J*. 2016;25(9):2898-2908.  
doi:10.1007/s00586-016-4542-0
26. Grant M, Epure LM, Salem O, et al. Development of a Large Animal Long-Term Intervertebral Disc Organ Culture Model That Includes the Bony Vertebrae for Grant, M., Epure, L. M., Salem, O., AlGarni, N., Ciobanu, O., Alaqeel, M., Antoniou, J., & Mwale, F. (2016). Development of a Large Animal . *Tissue Eng - Part C Methods*. 2016;22(7):636-643. doi:10.1089/ten.tec.2016.0049
27. Stannard JT, Edamura K, Stoker AM, et al. Development of a whole organ culture model for intervertebral disc disease. *J Orthop Transl*. 2016.  
doi:10.1016/j.jot.2015.08.002
28. Hartman RA, Bell KM, Debski RE, Kang JD, Sowa GA. Novel ex-vivo mechanobiological intervertebral disc culture system. *J Biomech*. 2012.  
doi:10.1016/j.jbiomech.2011.10.036
29. Jim B, Steffen T, Moir J, Roughley PJ, Haglund L. Development of an intact intervertebral disc organ culture system in which degeneration can be induced as a prelude to studying repair potential. *Eur Spine J*. 2011;20(8):1244-1254;
30. Xing Y, Zhang P, Zhang Y, et al. A multi-throughput mechanical loading system for mouse intervertebral disc. *J Mech Behav Biomed Mater*. 2020.  
doi:10.1016/j.jmbbm.2020.103636
31. Dai J, Xing Y, Xiao L, et al. Microfluidic Disc-on-a-Chip Device for Mouse Intervertebral Disc - Pitching a Next-Generation Research Platform to Study Disc

- Degeneration. *ACS Biomater Sci Eng*. 2019. doi:10.1021/acsbiomaterials.8b01522
32. Wu X, Liao Z, Wang K, et al. Targeting the IL-1  $\beta$  / IL-1Ra pathways for the aggregation of human islet amyloid polypeptide in an ex vivo organ culture system of the intervertebral disc. *Exp Mol Med*. 2019. doi:10.1038/s12276-019-0310-7
33. Koerner JD, Markova DZ, Schroeder GD, et al. The effect of substance P on an intervertebral disc rat organ culture model. *Spine (Phila Pa 1976)*. 2016. doi:10.1097/BRS.0000000000001676
34. McKee C, Beeravolu N, Brown C, Perez-Cruet M, Chaudhry GR. Mesenchymal stem cells transplanted with self-assembling scaffolds differentiated to regenerate nucleus pulposus in an ex vivo model of degenerative disc disease. *Appl Mater Today*. 2020. doi:10.1016/j.apmt.2019.100474
35. Li Z, Gehlen Y, Heizmann F, et al. Preclinical ex-vivo Testing of Anti-inflammatory Drugs in a Bovine Intervertebral Degenerative Disc Model. *Front Bioeng Biotechnol*. 2020;8(June):1-23. doi:10.3389/fbioe.2020.00583
36. Zhou Z, Zeiter S, Schmid T, et al. Effect of the CCL5-Releasing Fibrin Gel for Intervertebral Disc Regeneration. *Cartilage*. 2020;11(2):169-180. doi:10.1177/1947603518764263
37. Rosenzweig DH, Fairag R, Mathieu AP, et al. Thermoreversible hyaluronan-hydrogel and autologous nucleus pulposus cell delivery regenerates human intervertebral discs in an ex vivo, physiological organ culture model. *Eur Cells Mater*. 2018;36:200-217. doi:10.22203/eCM.v036a15
38. Frauchiger DA, Chan SCW, Benneker LM, Gantenbein B. Intervertebral disc damage models in organ culture: a comparison of annulus fibrosus cross-incision versus punch model under complex loading. *Eur Spine J*. 2018. doi:10.1007/s00586-018-5638-5
39. Illien-Jünger S, Gantenbein-Ritter B, Grad S, et al. The combined effects of limited

- nutrition and high-frequency loading on intervertebral discs with endplates. *Spine (Phila Pa 1976)*. 2010;35(19):1744-1752. doi:10.1097/BRS.0b013e3181c48019
40. Gantenbein B, Grunhagen T, Lee CR, Van Donkelaar CC, Alini M, Ito K. An in vitro organ culturing system for intervertebral disc explants with vertebral endplates: A feasibility study with ovine caudal discs. *Spine (Phila Pa 1976)*. 2006;31(23):2665-2673. doi:10.1097/01.brs.0000244620.15386.df
41. Peeters M, Van Rijn S, Vergroesen PPA, et al. Bioluminescence-mediated longitudinal monitoring of adipose-derived stem cells in a large mammal ex vivo organ culture. *Sci Rep*. 2015. doi:10.1038/srep13960
42. Shi J, Pang L, Jiao S. The response of nucleus pulposus cell senescence to static and dynamic compressions in a disc organ culture. *Biosci Rep*. 2018. doi:10.1042/BSR20180064
43. Beckstein JC, Sen S, Schaer TP, Vresilovic EJ, Elliott DM. Comparison of animal discs used in disc research to human lumbar disc: Axial compression mechanics and glycosaminoglycan content. *Spine (Phila Pa 1976)*. 2008;33(6):166-173. doi:10.1097/BRS.0b013e318166e001
44. Pattappa G, Li Z, Peroglio M, Wismer N, Alini M, Grad S. Diversity of intervertebral disc cells: Phenotype and function. *J Anat*. 2012. doi:10.1111/j.1469-7580.2012.01521.x
45. Du J, Pfannkuche J, Lang G, et al. Proinflammatory intervertebral disc cell and organ culture models induced by tumor necrosis factor alpha. *JOR Spine*. 2020;(May):1-12. doi:10.1002/jsp2.1104
46. Malda J, van Blitterswijk C, van Geffen M, Martens DE, Tramper J, Riesle J. Low oxygen tension stimulates the redifferentiation of dedifferentiate adult human nasal chondrocytes. *Osteoarthr Cartil*. 2004;12(4):306-313. doi:10.1016/j.joca.2003.12.001

47. Grimshaw MJ, Mason RM. Bovine articular chondrocyte function in vitro depends upon oxygen tension. *Osteoarthr Cartil.* 2000;8(5):386-392.  
doi:10.1053/joca.1999.0314
48. Scotti C, Osmokrovic A, Wolf F, et al. Response of human engineered cartilage based on articular or nasal chondrocytes to interleukin-1 $\beta$  and low oxygen. *Tissue Eng - Part A.* 2012;18(3-4):362-372. doi:10.1089/ten.tea.2011.0234
49. Naqvi SM, Buckley CT. Extracellular matrix production by nucleus pulposus and bone marrow stem cells in response to altered oxygen and glucose microenvironments. *J Anat.* 2015;227(6):757-766. doi:10.1111/joa.12305
50. Wuertz K, Godburn K, Neidlinger-Wilke C, Urban J, Iatridis JC. Behavior of mesenchymal stem cells in the chemical microenvironment of the intervertebral disc. *Spine (Phila Pa 1976).* 2008;33(17):1843-1849. doi:10.1097/BRS.0b013e31817b8f53
51. Wuertz K, Godburn K, Iatridis JC. MSC response to pH levels found in degenerating intervertebral discs. *Biochem Biophys Res Commun.* 2009;379(4):824-829.  
doi:10.1016/j.bbrc.2008.12.145
52. Naqvi SM, Buckley CT. Bone marrow stem cells in response to intervertebral disc-like matrix acidity and oxygen concentration implications for cell-based regenerative therapy. *Spine (Phila Pa 1976).* 2016;41(9):743-750.  
doi:10.1097/BRS.0000000000001314
53. Bibby S, Jones D a, Ripley RM, Urban JPG. Metabolism of the intervertebral disc: effects of low levels of oxygen, glucose, and pH on rates of energy metabolism of bovine nucleus pulposus cells. *Spine (Phila Pa 1976).* 2005;30(5):487-496;
54. Bartels EM, Fairbank JCT, Winlove PC, Urban JPG. Oxygen and lactate concentrations measured in vivo in the intervertebral discs of patients with scoliosis and back pain. *Spine (Phila Pa 1976).* 1998;23(1):1-8;



55. Sélard E, Shirazi-Adl A, Urban JPG. Finite element study of nutrient diffusion in the human intervertebral disc. *Spine (Phila Pa 1976)*. 2003;28(17):1945-1953;
56. Magnier C, Boiron O, Wendling-Mansuy S, Chabrand P, Deplano V. Nutrient distribution and metabolism in the intervertebral disc in the unloaded state: A parametric study. *J Biomech*. 2009;42(2):100-108;
57. Soukane DM, Shirazi-Adl A. Investigation of solute concentrations in a 3D model of intervertebral disc. *Eur Spine J*. 2009;18(2):254-262;
58. Shirazi-Adl A, Taheri M, Urban JPG. Analysis of cell viability in intervertebral disc: Effect of endplate permeability on cell population. *J Biomech*. 2010;43(7):1330-1336;
59. Jackson AR, Huang C-YC, Gu WY. Effect of endplate calcification and mechanical deformation on the distribution of glucose in intervertebral disc: a 3D finite element study. *Comput Methods Biomech Biomed Engin*. 2011;14(2):195-204;
60. Jackson AR, Huang C-YC, Brown MD, Gu WY. 3D Finite Element Analysis of Nutrient Distributions and Cell Viability in the Intervertebral Disc: Effects of Deformation and Degeneration. *J Biomech Eng*. 2011;133(9). doi:10.1115/1.4004944
61. Zhu Q, Jackson AR, Gu WY. Cell viability in intervertebral disc under various nutritional and dynamic loading conditions: 3d Finite element analysis. *J Biomech*. 2012;45(16):2769-2777;
62. Galbusera F, Mietsch A, Schmidt H, Wilke HJ, Neidlinger-Wilke C. Effect of intervertebral disc degeneration on disc cell viability: a numerical investigation. *Comput Methods Biomech Biomed Engin*. 2013;16(3):328-337;
63. Wu Y, Cisewski SE, Sachs BL, Yao H. Effect of cartilage endplate on cell based disc regeneration: a finite element analysis. *Mol Cell Biomech*. 2015;10(2):159-182;
64. Bibby S, Urban JPG. Effect of nutrient deprivation on the viability of intervertebral disc cells. *Eur Spine J*. 2004;13(8):695-701;

65. Ishihara H, Urban JPG. Effects of low oxygen concentrations and metabolic inhibitors on proteoglycan and protein synthesis rates in the intervertebral disc. *J Orthopaedic Res.* 1999;17(6):829-835;
66. Johnson ZI, Schoepflin ZR, Choi H, Shapiro IM, Risbud M V. Disc in flames: Roles of TNF- $\alpha$  and IL-1 $\beta$  in intervertebral disc degeneration. *Eur Cells Mater.* 2015;30:104-117. doi:10.22203/eCM.v030a08
67. Gilbert HTJ, Hodson NW, Baird P, Richardson SM, Hoyland JA. Acidic pH promotes intervertebral disc degeneration: Acid-sensing ion channel -3 as a potential therapeutic target. *Sci Rep.* 2016;6(1):37360. doi:10.1038/srep37360
68. Richardson SM, Knowles R, Tyler J, Mobasher A, Hoyland JA. Expression of glucose transporters GLUT-1, GLUT-3, GLUT-9 and HIF-1 $\alpha$  in normal and degenerate human intervertebral disc. *Histochem Cell Biol.* 2008;129(4):503-511. doi:10.1007/s00418-007-0372-9
69. Mwale F, Ciobanu I, Giannitsios D, Roughley PJ, Steffen T, Antoniou J. Effect of Oxygen Levels on Proteoglycan Synthesis by Intervertebral Disc Cells. *Spine (Phila Pa 1976).* 2011;36(2):131-138. doi:10.1097/BRS.0b013e3181d52b9e
70. Pfannkuche J, Guo W, Cui S, et al. Intervertebral disc organ culture for the investigation of disc pathology and regeneration – benefits , limitations , and future directions of bioreactors. *Connect Tissue Res.* 2019;00(00):1-18. doi:10.1080/03008207.2019.1665652
71. Walter BA, Korecki CL, Purmessur D, Roughley PJ, Michalek AJ, Iatridis JC. Complex loading affects intervertebral disc mechanics and biology. *Osteoarthr Cartil.* 2011;19(8):1011-1018. doi:10.1016/j.joca.2011.04.005
72. Walter BA, Illien-Jünger S, Nasser P, Hecht AC, Iatridis JC. Development and validation of a bioreactor system for dynamic loading and mechanical characterization

- of whole human intervertebral discs in organ culture. *J Biomech.* 2014;47(9):2095-2101;
73. Walter BA, Likhitpanichkul M, Illien-Junger S, Roughley PJ, Hecht AC, Iatridis JC. TNF $\alpha$  transport induced by dynamic loading alters biomechanics of intact intervertebral discs. *PLoS One.* 2015;10(3):1-16. doi:10.1371/journal.pone.0118358
74. Gantenbein B, Frauchiger DA, May RD, Bakirci E, Rohrer U, Grad S. Developing bioreactors to host joint-derived tissues that require mechanical stimulation. *Encycl Tissue Eng Regen Med.* 2019;1-3(March):261-280. doi:10.1016/B978-0-12-801238-3.65611-8
75. O'Connell GD, Vresilovic EJ, Elliott DM. Comparison of Animals Used in Disc Research to Human Lumbar Disc Geometry. *Spine (Phila Pa 1976).* 2007;32(3):328-333;
76. Huang C-YC, Gu WY. Effects of mechanical compression on metabolism and distribution of oxygen and lactate in intervertebral disc. *J Biomech.* 2008;41(6):1184-1196;
77. Huang C-YC, Yuan T-Y, Jackson AR, Hazbun L, Fraker C, Gu WY. Effects of Low Glucose Concentrations on Oxygen Consumption Rates of Intervertebral Disc Cells. *Spine (Phila Pa 1976).* 2007;32(19):2063-2069;
78. Soukane DM, Shirazi-Adl A, Urban JPG. Analysis of Nonlinear Coupled Diffusion of Oxygen and Lactic Acid in Intervertebral Discs. *J Biomech Eng.* 2005;127(12):1121-1126;
79. Li Z, Lang G, Karfeld-Sulzer LS, et al. Heterodimeric BMP-2/7 for nucleus pulposus regeneration—In vitro and ex vivo studies. *J Orthop Res.* 2017;35(1):51-60. doi:10.1002/jor.23351
80. Li Z, Lang G, Chen X, et al. Polyurethane scaffold with in situ swelling capacity for

- nucleus pulposus replacement. *Biomaterials*. 2016;84:196-209.  
doi:10.1016/j.biomaterials.2016.01.040
81. Walter BA, Purmessur D, Moon A, et al. Reduced tissue osmolarity increases trpv4 expression and pro-inflammatory cytokines in intervertebral disc cells. *Eur Cells Mater*. 2016;32:123-136. doi:10.22203/eCM.v032a08
82. Illien-Jünger S, Lu Y, Purmessur D, et al. Detrimental effects of discectomy on intervertebral disc biology can be decelerated by growth factor treatment during surgery: A large animal organ culture model. *Spine J*. 2014;14(11):2724-2732.  
doi:10.1016/j.spinee.2014.04.017
83. Beatty AM, Bowden AE, Bridgewater LC. Functional Validation of a Complex Loading Whole Spinal Segment Bioreactor Design. *J Biomech Eng*. 2016;138(6):1-4.  
doi:10.1115/1.4033546
84. Pattappa G, Peroglio M, Sakai D, et al. CCL5/rantes is a key chemoattractant released by degenerative intervertebral discs in organ culture. *Eur Cells Mater*. 2014;27:124-136. doi:10.22203/eCM.v027a10
85. Frauchiger DA, May RD, Bakirci E, et al. Genipin-enhanced fibrin hydrogel and novel silk for intervertebral disc repair in a loaded bovine organ culture model. *J Funct Biomater*. 2018;9(3). doi:10.3390/jfb9030040
86. Chan SCW, Walser J, Ferguson SJ, Gantenbein B. Duration-dependent influence of dynamic torsion on the intervertebral disc: an intact disc organ culture study. *Eur Spine J*. 2015;24(11):2402-2410. doi:10.1007/s00586-015-4140-6
87. Chan SCW, Walser J, Käppeli P, Shamsollahi MJ, Ferguson SJ, Gantenbein-Ritter B. Region Specific Response of Intervertebral Disc Cells to Complex Dynamic Loading: An Organ Culture Study Using a Dynamic Torsion-Compression Bioreactor. *PLoS One*. 2013;8(8):1-11. doi:10.1371/journal.pone.0072489

88. Nachemson A. Intradiscal measurements of pH in patients with lumbar rhizopathies. *Acta Orthop.* 1969;40(1):23-42. doi:10.3109/17453676908989482
89. Nachemson A, Lewin T, Maroudas A, Freeman MAR. In vitro diffusion of dye through the end-plates and the annulus fibrosus of human lumbar inter-vertebral discs. *Acta Orthop.* 1970;41(6):589-607. doi:10.3109/17453677008991550
90. Roberts S, Urban JPG, Evans H, Eisenstein SM. Transport Properties of the Human Cartilage Endplate in Relation to Its Composition and Calcification. *Spine (Phila Pa 1976).* 1996;21(4):415-420.
91. Maroudas A, Stockwell R, Nachemson A, Urban JPG. Factors involved in the nutrition of the human lumbar intervertebral disc: cellularity and diffusion of glucose in vitro. *J Anat.* 1975;120(1):113-130;
92. Urban JPG, Maroudas A. The measurement of fixed charge density in the intervertebral disc. *Biochim Biophys Acta.* 1979;586:166-178;
93. Jackson AR, Yuan T-Y, Huang C-YC, Travascio F, Gu WY. Effect of Compression and Anisotropy on the Diffusion of Glucose in Annulus Fibrosus. *Spine (Phila Pa 1976).* 2008;33(1):1-7;
94. Jackson AR, Yuan T-Y, Huang C-YC. Nutrient Transport in Human Annulus Fibrosus is Affected by Compressive Strain and Anisotropy. *Ann Biomed Eng.* 2012;40(12):1-8;
95. Boubriak OA, Watson N, Sivan SS, Stubbens N, Urban JPG. Factors regulating viable cell density in the intervertebral disc: Blood supply in relation to disc height. *J Anat.* 2013;222(3):341-348;
96. Zhou Z, Cui S, Du J, et al. One strike loading organ culture model to investigate the post-traumatic disc degenerative condition. *J Orthop Transl.* 2020;(July). doi:10.1016/j.jot.2020.08.003
97. Urban JPG, Holm S. Nutrition of the intervertebral disc: effect of fluid flow on solute

- transport. *Clin Orthop Relat Res.* 1982;(170):296-302;
98. Miyazaki T, Kobayashi S, Takeno K, Meir A, Urban JPG, Baba H. A Phenotypic Comparison of Proteoglycan Production of Intervertebral Disc Cells Isolated from Rats, Rabbits, and Bovine Tails; Which Animal Model is Most Suitable to Study Tissue Engineering and Biological Repair of Human Disc Disorders? *Tissue Eng Part A.* 2009;15(12):3835-3846. doi:10.1089/ten.tea.2009.0250
99. Cisewski SE, Wu Y, Damon BJ, Sachs BL, Kern MJ, Yao H. Comparison of Oxygen Consumption Rates of Nondegenerate and Degenerate Human Intervertebral Disc Cells. *Spine (Phila Pa 1976).* 2018;43(2):E60-E67.  
doi:10.1097/BRS.0000000000002252
100. Baumgartner L, Reagh JJ, González Ballester M, Noailly J. Simulating intervertebral disc cell behaviour within 3D multifactorial environments. *Bioinformatics.* 2020:0-1.  
doi:10.1093/bioinformatics/xxxxxx
101. Suhaimi H, Wang S, Das DB. Glucose diffusivity in cell culture medium. *Chem Eng J.* 2015. doi:10.1016/j.cej.2015.01.130
102. Figueiredo L, Pace R, D'Arros C, et al. Assessing glucose and oxygen diffusion in hydrogels for the rational design of 3D stem cell scaffolds in regenerative medicine. *J Tissue Eng Regen Med.* 2018;12(5):1238-1246. doi:10.1002/term.2656
103. Ribeiro ACF, Ortona O, Simões SMN, et al. Binary mutual diffusion coefficients of aqueous solutions of sucrose, lactose, glucose, and fructose in the temperature range from (298.15 to 328.15) K. *J Chem Eng Data.* 2006. doi:10.1021/je0602061
104. Wenger R, Kurtcuoglu V, Scholz C, Marti H, Hoogewijs D. Frequently asked questions in hypoxia research. *Hypoxia.* 2015;35. doi:10.2147/hp.s92198